

1 **Performance of bias correction schemes for CMORPH**  
2 **rainfall estimates in the Zambezi River Basin**

3 **Webster Gumindoga<sup>12</sup>, Tom. H.M. Rientjes<sup>1</sup>, Alemseged.T. Haile<sup>3</sup>, Hodson Makurira<sup>2</sup> and Paolo**  
4 **Reggiani<sup>4</sup>**

5 *<sup>1</sup>Faculty ITC, University of Twente, The Netherlands*

6 *<sup>2</sup>Civil Engineering Department, University of Zimbabwe, Zimbabwe*

7 *<sup>3</sup>International Water Management Institute (IWMI), Ethiopia*

8 *<sup>4</sup>University of Siegen, Germany*

9

10 *Email of corresponding author: [w.gumindoga@utwente.nl](mailto:w.gumindoga@utwente.nl)*  
11

---

12

13

14

15

16

17 Submission: 1 March 2018

18

19

20

21

22

23 *Email of corresponding author: [w.gumindoga@utwente.nl](mailto:w.gumindoga@utwente.nl)*  
24

25

26

27

28

29

30

31 **Abstract**

32 Satellite Rainfall Estimates (SRE) are prone to bias as they are indirect derivatives of the  
33 visible, infrared, and/or microwave cloud properties, hence SREs need correction. We evaluate  
34 the influence of elevation and distance from large scale open water bodies on bias for Climate  
35 Prediction Center-MORPHing (CMORPH) rainfall estimates in the Zambezi Basin. The  
36 effectiveness of five linear/non-linear and time-space variant/invariant bias correction schemes  
37 was evaluated for daily rainfall estimates and climatic seasonality. We used daily time series  
38 (1999-2013) from 52 gauge stations and for CMORPH SREs for the Zambezi Basin. To  
39 evaluate effectiveness of the bias correction techniques, spatial cross-validation was  
40 applied based on 8 stations whereas temporal cross-validation was based on the 1998-1999  
41 CMORPH time series. For correction, the Spatio-temporal Bias (STB) and Elevation Zone bias  
42 (EZ) schemes are more effective in removing bias. STB improved the correlation coefficient  
43 and Nash Sutcliffe efficiency by 50 % and 53 % respectively and reduced the root mean squared  
44 difference and relative bias by 25 % and 33 % respectively. Paired t-tests showed that there is  
45 no significant difference ( $p < 0.05$ ) in the daily means of CMORPH against gauge estimates  
46 after bias correction, whereas ANOVA post-hoc tests reveal that the STB and EZ bias  
47 correction schemes are preferable. Corrected CMORPH rainfall reveal an overestimation of  
48 very light rainfall ( $< 2.5$  mm/day) and underestimation of very heavy rainfall ( $> 20.0$  mm/day)  
49 for all five correction schemes. Bias is best reduced for rainfall rates of 0.0-2.5 and 5.0-10.0  
50 mm/day, a result also shown through quantile-quantile (q-q) plots. Bias removal proved to be  
51 more effective in the wet season than in the dry. The spatial cross-validation approach revealed  
52 that the majority of the bias correction schemes removed bias by 28 %. The temporal cross-  
53 validation approach showed in some instances the effectiveness of the bias correction schemes.  
54 Taylor diagrams show that station elevation and distance from large scale open water bodies  
55 have an influence on CMORPH performance. Findings of this study show the importance of  
56 applying bias correction to satellite rainfall estimates before application in hydrological  
57 analyses.

58

59 **Keywords:** *distance zone, elevation zone, satellite rainfall estimates, spatio-temporal bias,*  
60 *Taylor diagram*

61

62

## 63 **1. Introduction**

64

65 Correction schemes for rainfall estimates are developed for climate models (Maraun,  
66 2016;Grillakis et al., 2017;Switanek et al., 2017), for radar approaches (Cecinati et al.,  
67 2017;Yoo et al., 2014) and for satellite based, multi-sensor approaches (Najmaddin et al.,  
68 2017;Valdés-Pineda et al., 2016). In this study focus is on satellite rainfall estimates (SREs) to  
69 improve reliability in water resource applications.

70

71 Studies in satellite based rainfall estimation show that estimates are prone to systematic and  
72 random errors (Gebregiorgis et al., 2012;Habib et al., 2014;Shrestha, 2011;Tefsagiorgis et al.,  
73 2011;Vernimmen et al., 2012;Woody et al., 2014) Errors result primarily from the indirect  
74 estimation of rainfall from visible (VIS), infrared (IR), and/or microwave (MW) based satellite  
75 remote sensing of cloud properties (Pereira Filho et al., 2010;Romano et al., 2017). Systematic  
76 errors in SREs commonly are referred to as bias, which is a measure that indicates the  
77 accumulated difference between rain gauge observations and SREs. Bias in SREs is expressed  
78 for rainfall depth (Habib et al., 2012b), rain rate (Haile et al., 2013) and frequency at which  
79 rain rates occur (Khan et al., 2014). Bias may be negative or positive where negative bias  
80 indicates underestimation whereas positive bias indicates overestimation (Liu, 2015;Moazami  
81 et al., 2013).

82

83 Recent studies on CMORPH (Wehbe et al., 2017;Jiang et al., 2016;Liu et al., 2015;Haile et  
84 al., 2015) reveal that accuracy of CMORPH satellite rainfall varies across different regions,  
85 but causes are not directly indentifiable. As such correction schemes serve to reduce systematic  
86 errors and to improve aplicability of SREs. Correction schemes rely on assumptions that adjust  
87 errors in space and/or time (Habib et al., 2014). Some correction schemes consider correction  
88 only for spatial distributed patterns in bias, commonly known as space variant/invariant.  
89 Approaches that correct for spatially averaged bias have roots in radar rainfall estimation (Seo  
90 et al., 1999) but are unsuitable for large scale basins ( $> 5,000 \text{ km}^2$ ) where rainfall may  
91 substantially vary in space (Habib et al., 2014). Studies by Tefsagiorgis et al. (2011) in  
92 Oklahoma (USA) and Müller and Thompson (2013) in Nepal concluded that space variant  
93 correction schemes are more effective in reducing CMORPH and TRMM bias than space  
94 invariant correction schemes. In a study conducted in the Upper Blue Nile basin in Ethiopia,  
95 Bhatti et al. (2016) show that CMORPH bias correction is most effective when correction is  
96 for a 7 day sequential window.

97

98 Bias correction schemes based on regression techniques have reported distortion of frequency  
99 of rainfall rates (Ines and Hansen, 2006;Marcos et al., 2018). Multiplicative shift procedures  
100 tend to adjust SRE rainfall rates, but Ines and Hansen (2006) reported that they do not correct  
101 systematic errors in rainfall frequency of climate models. Non-multiplicative bias correction

102 schemes preserve the timing of rainfall within a season (Fang et al., 2015; Hempel et al., 2013).  
103 Studies that have applied non-linear bias correction schemes such as Power Function report  
104 correction of extreme values (depth, rate and frequency) thus mitigating the underestimation  
105 and overestimation of CMORPH rainfall (Vernimmen et al., 2012). The study by Tian (2010)  
106 in the United States noted that the Bayesian (likelihood) analysis techniques are found to over-  
107 adjust both light and heavy satellite rainfall towards moderate CMORPH rainfall.

108

109 Bias often exhibits a topographic and latitudinal dependency as, for instance, shown for the  
110 National Oceanic and Atmospheric Administration (NOAA) Climate Prediction Center-  
111 MORPHing (CMORPH) product in the Nile Basin (Bitew et al., 2011; Habib et al., 2012a; Haile  
112 et al., 2013). For Southern Africa, Thorne et al. (2001), Dinku et al. (2008) and Meyer et al.  
113 (2017) show that bias in rainfall rate and frequency can be related to location, topography, local  
114 climate and season. First studies in the Zambezi Basin (Southern Africa) on SREs show  
115 evidence that necessitates correction of SREs. For example, Cohen Liechti (2012) show bias  
116 in CMORPH SREs for daily rainfall and for accumulated rainfall at monthly scale. Matos et  
117 al. (2013), Thiemig et al. (2012) and Toté et al. (2015) show that bias in rainfall depth at time  
118 intervals ranging from daily to monthly varies across geographical domains in the Zambezi  
119 Basin and may be as large as  $\pm 50\%$ . Besides topographic effects, rainfall is affected by  
120 presence of large scale open water bodies which influences surface or atmospheric properties  
121 (Haile et al., 2009; Rientjes et al., 2013a). As such, SREs may be affected as well as suggested  
122 in (Rientjes et al., 2013b).

123

124 For less developed areas such as in the Zambezi Basin that is selected for this study,  
125 applications of SREs are limited. This is despite the strategic importance of the basin in  
126 providing water to over 30 million people (World Bank, 2010a). An exception is the study by  
127 Beyer et al. (2014) on correction of the TRMM-3B42 product for agricultural purposes in the  
128 Upper Zambezi Basin. Studies (Cohen Liechti et al., 2012; Meier et al., 2011) on use of SREs  
129 in the Zambezi River Basin mainly focused on accuracy assessment of the SREs using standard  
130 statistical indicators with little or no effort to perform bias correction despite the evidence of  
131 errors in these products. The use of uncorrected satellite rainfall is reported for hydrological  
132 modelling in the Nile Basin (Bitew and Gebremichael, 2011) and Zambezi Basin (Cohen  
133 Liechti et al., 2012), respectively, and for drought monitoring in Mozambique (Toté et al.,  
134 2015). The above studies highlight the need to correct SREs. The selection of CMORPH  
135 satellite rainfall for this study is based on successful applications of bias corrected CMORPH  
136 estimates in African basins for hydrological modelling (Habib et al., 2014) and flood  
137 predictions in West Africa (Thiemig et al., 2013). In first publications on CMORPH, Joyce et  
138 al. (2004) describe CMORPH as a gridded precipitation product that estimates rainfall with  
139 information derived from IR data and MW data. CMORPH combines the retrieval accuracy of  
140 passive MW estimates with IR measurements which are available at high temporal resolution  
141 but with low accuracy. The important distinction between CMORPH and other merging

142 methods is that the IR data are not used for rainfall estimation but used only to propagate  
143 rainfall features that have been derived from microwave data. The flexible ‘morphing’  
144 technique is applied to modify the shape and rate of rainfall patterns. CMORPH is operational  
145 since 2002 for which data is available at the CPC of the National Centers for Environmental  
146 Prediction (NCEP) (after <http://www.ncep.noaa.gov/>). Recent publications on CMORPH in  
147 African basins exist (Wehbe et al., 2017;Koutsouris et al., 2016;Jiang et al., 2016;Haile et al.,  
148 2015). However CMORPH data applicability after bias correction in the semi-arid Zambezi  
149 Basin has not been fully investigated. Therefore, evaluating and finding the appropriate bias  
150 correction method for the data is necessary for water resources management in the basin.

151

152 In this study we use daily CMORPH and rain gauge data for Upper, Middle, and Lower  
153 Zambezi basins to (1) evaluate if performance of CMORPH rainfall is affected by elevation  
154 and distance from large scale open water bodies (2) evaluate the effectiveness of linear/non-  
155 linear and time-space variant/invariant bias correction schemes and (3) assess the performance  
156 of bias correction schemes to represent different rainfall rates and climate seasonality. Analysis  
157 serve to improve reliability of SREs applications in water resource applications in the Zambezi  
158 basin such as in drought analysis, flood prediction, weather forecasting and rainfall runoff  
159 modeling

160

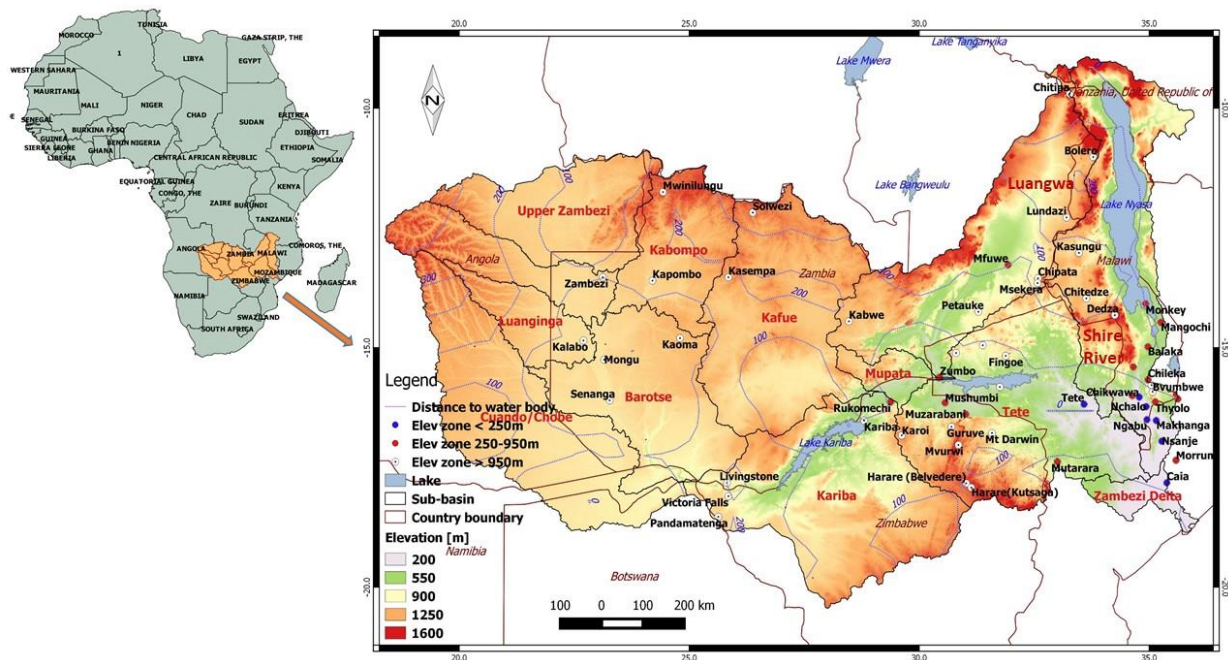
## 161 **2. Study area**

162 The Zambezi River is the fourth-longest river (~2,574 km) in Africa with basin area of  
163 ~1,390,000 km<sup>2</sup> (~4 % of the African continent). The river drains into the Indian Ocean and  
164 has mean annual discharge of 4,134 m<sup>3</sup>/s (World Bank, 2010a). The river has its source in  
165 Zambia with basin boundaries in Angola, Namibia Botswana, Zambia, Zimbabwe and  
166 Mozambique (Fig. 1). The basin is characterized by considerable differences in elevation and  
167 topography, distinct climatic seasons and presence of large scale open water bodies and, as  
168 such, makes the basin well suited for this study. The basin is divided into three subbasins i.e.,  
169 the Lower Zambezi comprising the Tete, Lake Malawi/Shire, and Zambezi Delta basins, the  
170 Middle Zambezi comprising the Kariba, Mupata, Kafue, and Luangwa basins, and the Upper  
171 Zambezi comprising the Kabompo, Lungwebungo, Luanginga, Barotse, and Cuando/Chobe  
172 basins (Beilfuss, 2012).

173

174 The elevation of the Zambezi basin ranges from < 200 m (for some parts of Mozambique) to  
175 >1500 m above sea level (for some parts of Zambia). Large scale open water bodies in and  
176 around the basin are Kariba, Cabora Bassa, Bangweulu, Chilwa and Nyasa. The Indian Ocean  
177 is to the east of Mozambique. Typical landcover types are woodland, grassland, water surfaces  
178 and cropland (Beilfuss et al., 2000). The basin is characterized by high annual rainfall (>1,400  
179 mm/yr) in the northern and north-eastern areas but low annual rainfall (<500 mm/yr) in the  
180 southern and western parts (World Bank, 2010b). Due to this rainfall distribution, northern  
181 tributaries in the Upper Zambezi subbasin contribute 60 % of the mean annual discharge

182 (Tumbare, 2000). The river and its tributaries are subject to seasonal floods and droughts that  
 183 have devastating effects on the people and economies of the region, especially the poorest  
 184 members of the population (Tumbare, 2005). It is not uncommon to experience both floods and  
 185 droughts within the same hydrological year.  
 186



187 Figure 1: Zambezi River Basin from Africa with sub basins, major lakes, rivers, elevation, and locations and names of the 60  
 188 rain gauging stations used in this study. The Euclidian distance (km) from large scale open water bodies is also shown.

189  
 190 **3. Materials and Methodology**

191  
 192 **3.1. Rainfall data**

193  
 194 **3.1.1. CMORPH**

195 For this study, time series of CMORPH rainfall images (1998-2013) at 8 km × 8 km, 30-minute  
 196 resolution were selected. Images are downloaded by means of the GeoNETCAST ISOD  
 197 toolbox of ILWIS GIS software (<http://52north.org/downloads/>). Half hourly estimates were  
 198 aggregated to daily totals to match the observation interval of gauge based daily rainfall .

199  
 200 **3.1.2. Rain gauge network**

201 Time series of daily rainfall from 66 stations were obtained from meteorological departments  
 202 in Botswana, Malawi, Mozambique, Zambia and Zimbabwe for stations that cover the study  
 203 area. All the stations are standard type raingauges with a measuring cylinder whose units of  
 204 measurement is millimetres (mm).

205  
 206 After screening, 6 stations with suspicious time series were removed to remain with 60 stations.  
 207 Some stations are affected by data gaps but the available time series are of sufficiently long

208 duration to serve the objectives of this study. Stations are irregularly distributed across the vast  
209 basin and are located at elevation between 3 m to 1575 m (Figure 1). The minimum, maximum  
210 and average distance between the rain gauges is 3.5 km (Zumbo in Mozambique-Kanyemba in  
211 Zimbabwe), 1570 km (Mwinilunga in Zambia-Marromeu in Mozambique) and 565 km  
212 respectively. This variation of distances provides a good spatial base for analysis in this study.  
213 . Stations are located between an elevation range of 3 m to 1600 masl. Distances to large scale  
214 open water bodies range between 5 km and 615 km. This allows us to evaluate if elevation and  
215 distance to large scale open water bodies affects CMORPH performance.

216

### 217 *3.1.3. Comparison of CMORPH and rain gauge estimates*

218 In this study, we compare rain gauge estimates at point scale to CMORPH satellite derived  
219 rainfall estimates at pixel scale (point-to-pixel). Comparison is at a daily time interval covering  
220 the period 1998-2013, following (Cohen Liechti et al., 2012; Dinku et al., 2008; Haile et al.,  
221 2014; Hughes, 2006; Tsidu, 2012; Worqlul et al., 2014) who report on point-to-pixel  
222 comparisons in African basins. We apply point-to-pixel comparison to rule out any aspect of  
223 interpolation error as a consequence of the low density network with unevenly distributed  
224 stations. , We refer to (Heidinger et al., 2012; Li and Heap, 2011; Tobin and Bennett, 2010; Yin  
225 et al., 2008) who report that interpolation introduces unreliability and uncertainty to pixel based  
226 rainfall estimates. Also, Worqlul et al. (2014) describe that for pixel-to-pixel comparison, there  
227 is demand for a well distributed rain gauge network that would not hamper accurate  
228 interpolation..

229

230

## 231 **3.2. Elevation and distance from large scale open water bodies**

232 Studies by (Habib et al., 2012a; Haile et al., 2009; Rientjes et al., 2013a) in the Nile Basin reveal  
233 that elevation and distance to large-scale open water bodies affect performance of SREs. To  
234 assess such influences, we classified the Zambezi Basin into 3 elevation zones for which the  
235 hierarchical cluster ‘within-groups linkage’ method in the Statistical Product and Service  
236 Solutions (SPSS) software was used. (Table 1).

237

238 Based on Euclidian distance to large-scale open water bodies, 4 arbitrary distance zones are  
239 defined to group stations (Table 1). A detailed description on the individual stations, their  
240 elevation and distance to large-scale open water bodies is provided in Appendix 1. The  
241 Advanced Spaceborne Thermal Emission and Reflection Radiometer (ASTER) based DEM of  
242 30 m resolution obtained from <http://gdem.ersdac.jpacesystems.or.jp/>, is used to represent  
243 elevation across the Zambezi Basin. The Euclidian distance of each rain gauge location to  
244 large-scale open water bodies is defined in a GIS environment through the distance calculation  
245 algorithm. Large-scale open water bodies are defined as perennial open water bodies with  
246 surface area > 700 km<sup>2</sup>.

247

248

Table 1: Elevation and distance from large scale open water bodies

Zone ID	Elevation (m)	No. of stations	Mean elevation of stations (m)
Zone 1	< 250	8	90
Zone 2	250-950	21	510
Zone 3	> 950	31	1140

Zone ID	Distance (km)	No. of stations	Mean distance to large-scale open water bodies (km)
Zone 1	< 10 km	4	5
Zone 2	10 - 50	10	35
Zone 3	50 - 100	18	80
Zone 4	> 100	28	275

249

### 250 3.3. Bias correction schemes

251

252 Bias correction schemes evaluated in this study are the Spatio-temporal bias (STB), Elevation  
 253 zone bias (EZ), Power transform (PT), Distribution transformation (DT), and the Quantile  
 254 mapping based on an empirical distribution (QME). The five schemes are chosen based on  
 255 merits documented in literature (Bhatti et al., 2016; Habib et al., 2014; Teutschbein and Seibert,  
 256 2013; Themeßl et al., 2012; Vernimmen et al., 2012), since we aim to correct while daily rainfall  
 257 variability is preserved. We note that findings on the performance of selected bias correction  
 258 schemes in literature do not allow for generalization but findings only apply to the respective  
 259 study domains (Wehbe et al., 2017; Jiang et al., 2016; Liu et al., 2015; Haile et al., 2015).

260 In the procedure to define a time window for bias correction we follow (Habib et al., 2014) and  
 261 (Bhatti et al.; 2016) who in the Lake Tana Basin (Ethiopia) carried out a sensitivity analysis on  
 262 moving time windows and on sequential time windows. Window lengths of 3 and 31 days are  
 263 tested. Findings indicated that a 7-day sequential time window is most appropriate but only  
 264 when a minimum of five rainy days were recorded within the 7-day window with a minimum  
 265 rainfall accumulation depth of 5 mm, otherwise no bias is estimated (i.e. a value of 1 applies  
 266 as bias correction factor). Preliminary tests in this study on 5 and 7-day moving and sequential  
 267 windows on 20 individual stations distributed over the three elevation zones indicates that the  
 268 7-day sequential approach is well applicable in the Zambezi Basin. As such the approach  
 269 was selected.

270

271 The bias correction factors are calculated using only rain days (rainfall  $\geq 1$  mm). Otherwise in  
 272 cases where both the gauge and satellite have zero values (RG=0 and CMORPH =0), correction  
 273 is not applied and the SRE value remains 0 mm/day.

274

275 Following Bhatti et al. (2016), we spatially interpolated the bias correction factors so that  
 276 factors are subsequently applied to all SRE pixels. For interpolation Universal Kriging was



277 applied. Thus to systematically correct all CMORPH estimates, station based bias factors for  
 278 each time window are spatially interpolated to arrive at spatial coverage across the study area  
 279 and to allow for comparison with other approaches.

280

### 281 3.3.1. Spatio-temporal bias correction (STB)

282 This linear bias correction scheme has its origin in the correction of radar based precipitation  
 283 estimates (Tefragiorgis et al., 2011) and downscaled precipitation products from climate  
 284 models. The CMOPRH daily rainfall estimates ( $S$ ) are multiplied by the bias correction factor  
 285 for the respective sequential time window for individual stations resulting in corrected  
 286 CMORPH estimates ( $STB$ ) in a temporally and spatially coherent manner (Equation [1]).

$$287 \quad STB = S \frac{\sum_{t=d}^{t=d-l} S(i,t)}{\sum_{t=d}^{t=d-l} G(i,t)} \quad [1]$$

288 Where:

289  $G$  = gauged rainfall estimate (mm/day)

290  $i$  = gauge number

291  $d$  = day number

292  $t$  = julian day number

293  $l$  = length of a time window for bias correction

294

295 The advantages of this bias correction scheme is that it is straightforward and easy to implement  
 296 due to its simplicity and modest data requirements. However, just like any multiplicative shift  
 297 procedures of bias correction, STB does not correct intensities and systematic errors in rainfall  
 298 frequency particularly the wet-day frequencies (Lenderink et al., 2007; Teutschbein and  
 299 Seibert, 2013).

300

### 301 3.3.2. Elevation zone bias correction (EZ)

302 This bias scheme is proposed in this study and aims at correcting satellite rainfall for elevation  
 303 influences. This method groups rain gauge stations into 3 elevation zones based on station  
 304 elevation. The grouping in this study is based on the hierarchical clustering technique, expert  
 305 knowledge about the study area but also guided by relevant past studies in the basin (e.g. World  
 306 Bank, 2010b;Beilfuss, 2012). Each zone has the same bias correction factor but differs across  
 307 the three zones. In the time domain bias factors vary following the 7-day sequential window  
 308 approach. The corrected CMORPH estimates ( $EZ$ ) at daily time interval are obtained by  
 309 multiplying the uncorrected CMOPRH daily rainfall estimates ( $S$ ) by the daily bias correction  
 310 factor of each elevation zone.

311

$$312 \quad EZ = S \frac{\sum_{t=d}^{t=d-l} \sum_{i=1}^{i=n} S(i,t)}{\sum_{t=d}^{t=d-l} \sum_{i=1}^{i=n} G(i,t)} \quad [2]$$

313

314 The merits of this bias correction scheme is that the effects of elevation on rainfall depth are  
315 accounted for. SREs often have difficulties in capturing rainfall events due to orographic effects  
316 and thus require elevation based correction.

317

### 318 3.3.3. Power transform (PT)

319 The non-linear PT bias correction scheme has its origin in studies of climate change impact  
320 {Lafon, 2013 #926}. (Vernimmen et al., 2012) show that the scheme could be applied to correct  
321 satellite rainfall estimates for use in hydrological modelling and drought monitoring. The PT  
322 method uses an exponential form to adjust the standard deviation of rainfall series. The daily  
323 bias corrected CMORPH rainfall (PT) for a pixel that overlays a station is obtained using  
324 equation:

325

$$326 \quad PT = aG(i,t)^b \quad [3]$$

327 Where:

328  $G$  = rain gauge estimate (mm/day)

329  $a$  = prefactor such that the mean of the transformed CMORPH values is equal to the mean  
330 of gauge estimates

331  $b$  = factor calculated such that for each rain gauge the coefficient of variation (CV) of  
332 CMORPH matches the gauge based counter parts

333  $i$  = gauge number

334  $t$  = day number

335

336 Optimized values for  $a$  and  $b$  are obtained through the generalized reduced gradient algorithm  
337 (Fylstra et al., 1998). Values for  $a$  and  $b$  vary for the 7-day time sequential window since  
338 correction is at daily time base. In the case of utilizing the PT method in a certain area (or for a  
339 certain period), the bias correction factor is spatially interpolated to result in comparable  
340 estimates with other bias correction schemes. The advantage of the bias scheme is that it adjusts  
341 extreme precipitation values in CMORPH estimates (Vernimmen et al., 2012). PT has reported  
342 limitations in correcting wet-day frequencies and intensities (Leander et al., 2008; Teutschbein  
343 and Seibert, 2013).

344

### 345 3.3.4. Distribution transformation (DT)

346 DT is an additive bias correction approach which has its origin in statistical downscaling of  
347 climate model data (Bouwer et al., 2004). The method transforms a statistical distribution  
348 function of daily CMORPH rainfall estimates to match the distribution by gauged rainfall  
349 estimates. The procedure to match the CMORPH distribution function to gauge rainfall based  
350 counter parts is described in equations [4-8]. The principle to matching is that the difference in  
351 the mean value and differences in the variance are corrected for, in the 7-day sequential  
352 window. First, the bias correction factor for the mean ( $DTu$ ) is determined by equation [4]:

353

$$354 \quad DT_u = \frac{G_u}{S_u} \quad [4]$$

355  $G_u$  and  $S_u$  are mean values of 7-day gauge and CMORPH rainfall estimates.

356

357 Secondly, the correction factor for the variance ( $DT\tau$ ) is determined by the quotient of the 7-  
358 day standard deviations,  $G\tau$  and  $S\tau$ , for gauge and CMORPH respectively.

359

$$360 \quad DT\tau = \frac{G\tau}{S\tau} \quad [5]$$

361

362 Once the correction factors which vary within a 7-day time sequential window are established,  
363 they are then applied to correct all daily CMORPH estimates ( $S$ ) through equation [6] to obtain  
364 corrected CMORPH rainfall estimate ( $DT$ ). The parameters  $DT_u$  and  $DT\tau$  are developed within  
365 a 7-day sequential window but correction is then at daily time intervals.

366

$$367 \quad DT = (S(i, t) - S_u)DT\tau + DT_u * S\tau \quad [6]$$

368 Uncorrected CMORPH daily values are returned if [6] results in negative values. The merit of  
369 this bias correction scheme is that it corrects wet-day frequencies and intensities. The  
370 disadvantage of this bias correction scheme is that adding the gauge based mean deviation to  
371 the satellite data destroys the physical consistency of the data. In addition, the method might  
372 result in the generation of too few rain days in the wet season, and sometimes the mean of daily  
373 intensities might be unrealistically corrected (Johnson and Sharma, 2011; Teutschbein and  
374 Seibert, 2013).

375

### 376 3.3.5. Quantile mapping based on an empirical distribution ( $QME$ )

377 This is a quantile based empirical-statistical error correction method with its origin in empirical  
378 transformation and bias correction of regional climate model-simulated precipitation (Themeßl  
379 et al., 2012). The method corrects CMORPH precipitation based on empirical cumulative  
380 distribution functions ( $ecdfs$ ) which are established for each 7-day time window and for each  
381 station. The bias corrected rainfall ( $QME$ ) using quantile mapping are expressed in terms of  
382 the empirical cumulative distribution function ( $ecdf$ ) and its inverse ( $ecdf^{-1}$ ). Parameters apply  
383 to a 7-day sequential window but correction is then at daily time interval with bias spatially  
384 averaged for the entire domain to allow for comparison with other approaches

385

$$386 \quad QME = ecdf_{obs}^{-1}(ecdf_{raw}(S(i, t))) \quad [7]$$

387

388 Where:

389  $ecdf_{obs}$  = empirical cumulative distribution function for the gauge based observation

390  $ecdf_{raw}$  = empirical cumulative distribution function for the uncorrected CMORPH

391

392 The advantage of this bias scheme is that it corrects quantiles and preserves the extreme  
 393 precipitation values (Thiemeßl et al., 2012). However, it also has its limitation due to the  
 394 assumption that both the observed and satellite rainfall follow the same proposed distribution,  
 395 which may introduce potential new biases.  
 396

### 397 **3.4. Rainfall rates and seasons**

398 To assess the performance of SREs for different classes of daily rainfall rates five classes are  
 399 defined which indicate: very light (< 2.5 mm/day), light (2.5-5.0), moderate (5.0-10.0 mm/day),  
 400 heavy (10.0-20.0 mm/day) and very heavy rainfall (> 20 mm/day).  
 401

402 Furthermore, gauge based estimates were divided into wet and dry seasonal periods to assess  
 403 the influence of seasonality on performance of bias correction schemes. The wet season in the  
 404 Zambezi Basin spans from October-March whereas the dry season spans from April-  
 405 September.  
 406

### 407 **3.5. Evaluation of CMORPH estimates**

408 Corrected and uncorrected CMORPH satellite rainfall estimates are evaluated with reference  
 409 to rain gauge estimates using statistics that measure systematic differences (i.e. percentage  
 410 bias and Mean Absolute Error (MAE)), measures of association (e.g. correlation coefficient  
 411 and Nash Sutcliffe Efficiency (NSE)) and random differences (e.g. standard deviation of  
 412 differences and coefficient of variation) (Haile et al., 2013). Bias is a measure of how the  
 413 satellite rainfall estimate deviates from the raingauge estimate, and the result is normalised by  
 414 the summation of the gauge values. A positive value indicates overestimation whereas a  
 415 negative value indicates underestimation. The correlation coefficient (ranging between +1 and  
 416 -1) represents the linear dependence of gauge and CMORPH data. MAE is the arithmetic  
 417 average of the absolute values of the differences between the daily gauge and CMORPH  
 418 satellite rainfall estimates. The MAE is zero if the rainfall estimates are perfect and increases  
 419 as discrepancies between the gauge and satellite become larger. NSE indicates how well the  
 420 satellite rainfall matches the raingauge observation and it ranges between -∞ and 1, with NSE  
 421 = 1 meaning a perfect fit (Nash and Sutcliffe, 1970).  
 422

423 Equations [8-11] apply.  
 424

$$425 \quad bias (\%) = \frac{\sum(S-G)}{\sum G} * 100 \quad [8]$$

$$426 \quad R = \frac{\sum(G-\bar{G})(S-\bar{S})}{\sqrt{\sum(G-\bar{G})^2}\sqrt{\sum(S-\bar{S})^2}} \quad [9]$$

$$427 \quad MAE = \frac{1}{n} \sum |S - G| \quad [10]$$

430

$$431 \quad NSE = \frac{\sum(G-S)^2}{\sum(G-\bar{G})^2} \quad [11]$$

432

433 Where:

434  $S$  = satellite rainfall estimates (mm/day)

435  $\bar{S}$  = mean of the satellite rainfall estimates (mm/day)

436  $G$  = rainfall estimates by a rain gauge (mm/day)

437  $\bar{G}$  = mean values of rainfall recorded by a rain gauge (mm/day)

438  $n$  = number of observations

439

### 440 **3.6. Test for differences of mean**

441 To detect significant differences between gauge and satellite rainfall (corrected and  
 442 uncorrected) and differences amongst the five bias correction methods described in Section  
 443 3.3, we apply paired t-test and analysis of variance (ANOVA) tests.

444

#### 445 *3.6.1. Paired t-tests*

446 A paired t-test was used to test whether there is a significant difference between raingauge,  
 447 uncorrected and bias corrected CMORPH satellite rainfall for the 52 raingauges. Results are  
 448 summarized for the Upper, Lower and Middle Zambezi. The paired t-test compares the mean  
 449 difference of the values to zero. It depends on the mean difference, the variability of the  
 450 differences and the number of data. The null hypothesis ( $H_0$ ) is that there is no difference in  
 451 mean gauge and satellite daily rainfall (uncorrected and bias corrected). If the p-value is less  
 452 than or equal 0.05 (5%), the result is deemed statistically significant, i.e., there is a significant  
 453 relationship between the gauge and satellite rainfall (Wilks, 2006;Field 2009).

454

#### 455 *3.6.2. Analysis of Variance (ANOVA) test*

456 The ANOVA-test aims to test whether there is a significant difference amongst the 5 bias  
 457 correction techniques. The Null hypothesis ( $H_0$ ) is that there are no differences amongst the  
 458 five bias correction schemes. We further determined which schemes differ significantly using  
 459 3 post-hoc tests, namely: Tukey HSD, Scheffe and the Bonferroni (Brown, 2005; Kucuk et al.,  
 460 2018). Results are summarized for the Upper, Lower and Middle Zambezi.

461

### 462 **3.7. Taylor diagram**

463 We apply a Taylor diagram to evaluate differences in data sets generated by respective bias  
 464 correction schemes by providing a summary of how well bias correction results match gauge  
 465 based estimates in terms of pattern, variability and magnitude of the variability. Visual  
 466 comparison of SRE performance is done by analysing how well patterns match each other in  
 467 terms of the Pearson's product-moment correlation coefficient ( $R$ ), root mean square difference  
 468 ( $E$ ), and the ratio of variances on a 2-D plot (Lo Conti et al., 2014;Taylor, 2001). The reason  
 469 that each point in the two-dimensional space of the Taylor diagram can represent the above

470 three different statistics simultaneously is that the centered pattern of root mean square  
471 difference ( $E^i$ ), and the ratio of variances are related by the following:

$$472 \quad 473 \quad E^i = \sqrt{\sigma_f^2 + \sigma_r^2 - 2\sigma_f\sigma_rR} \quad [12]$$

474  
475 Where:

476  $\sigma_f$  and  $\sigma_r$  = standard deviation of CMORPH and rain gauge rainfall, respectively.

477  
478 Development and applications of Taylor diagrams have roots in climate change studies  
479 (Smiatek et al., 2016; Taylor, 2001) but also has frequent applications in environmental model  
480 evaluation studies (Cuvelier et al., 2007; Dennis et al., 2010; Srivastava et al., 2015). Bhatti et  
481 al., (2016) propose the use of Taylor Diagrams for assessing effectiveness of SREs bias  
482 correction schemes. The most effective bias correction schemes will have data that lie near a  
483 point marked 'reference' on the x-axis, relatively high correlation coefficient and low root  
484 mean square difference. Bias correction schemes matching gauged based standard deviation  
485 have patterns that have the right amplitude.

### 486 487 **3.8. Quantile-quantile (q-q) plots**

488 A q-q plot is used to check if two datasets (in this case gauge vs CMORPH rainfall) can fit the  
489 same distribution (Wilks, 2006). A q-q plot is a plot of the quantiles of the first data set against  
490 the quantiles of the second data set. A 45-degree reference line is also plotted. If the satellite  
491 rainfall (corrected and uncorrected) has the same distribution as the rainguage, the points  
492 should fall approximately along this reference line. The greater the departure from this  
493 reference line, the greater the evidence for the conclusion that the bias correction scheme is  
494 less effective (NIST/SEMATECH, 2001).

495  
496 The main advantage of the q-q plot is that many distributional aspects can be simultaneously  
497 tested. For example, changes in symmetry, and the presence of outliers can all be detected from  
498 this plot.

### 499 500 **3.9. Cross validation of bias correction**

#### 501 502 *3.9.1. Spatial cross-validation*

503 The spatial cross-validation procedure (hold-out sample) applied in this study, involves the  
504 withdrawal of 8 in-situ stations from the sample of 60 when generating bias corrected SREs  
505 for all pixels across the study area.. Corrected SREs are then compared to the gauge estimates  
506 of the withdrawn stations to evaluate closeness of match. From the sample of 8 we selected 2  
507 stations in the < 250 m elevation zone, 3 stations in the 250-950 m zone and 3 stations in > 950  
508 m elevation zone. Stations selected have elevation close to the average elevation zone value  
509 and are centred in an elevation zone. This left us with 52 stations for applying the bias

510 correction methods and spatial interpolation. As performance indicators to evaluate results of  
511 cross-validation, we use the percentage bias, MAE, Correlation Coefficient and the estimated  
512 ratio which is obtained by dividing CMORPH rainfall totals and gauge based rainfall totals for  
513 the 1999-2013 period.

514

### 515 *3.9.2. Temporal cross-validation*

516 For evaluation of SREs in the time domain we followed (Gutjahr and Heinemann, 2013) and  
517 omitted rainfall estimates (both from gauge and satellite) for the 1998-1999 hydrological year  
518 to remain with 14 years for bias correction of SREs. Bias corrected estimates for 1998-1999  
519 are then evaluated against estimates for the 14 years that served as reference. For evaluation  
520 we use the percentage bias, MAE, Correlation Coefficient and the estimated ratio, that all are  
521 averaged for the Upper, Middle and Lower Zambezi but also for the wet and dry seasons.

522

523

## 524 **4. Results and Discussion**

525

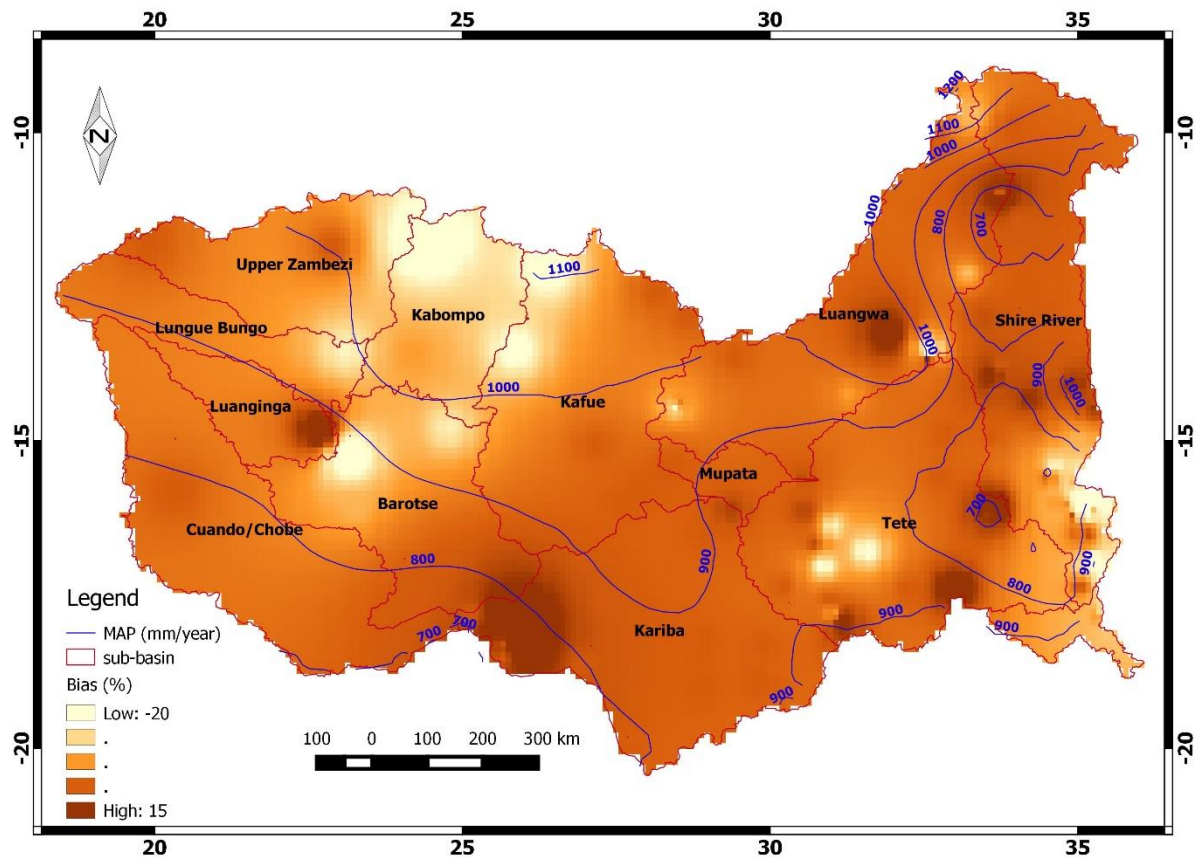
### 526 **4.1. Performance of uncorrected CMORPH rainfall**

527

528 The spatially interpolated values of bias (%) covering the Zambezi Basin are shown in Figure  
529 2. Areas in the central and western part of the basin have bias relatively close to zero suggesting  
530 good performance of the uncorrected CMORPH product. However large negative bias values  
531 (-20 %) are shown in the Upper Zambezi's high elevated areas such as Kabompo and northern  
532 Barotse Basin, in the south-eastern part of the basin such as Shire River Basin and in in the  
533 Lower Zambezi's downstream areas where the Zambezi River enters the Indian Ocean.  
534 CMORPH overestimates rainfall locally in Kariba, Luanginga, and Luangwa basins by positive  
535 bias values. As such CMORPH estimates do not consistently provide results that match gauge  
536 observations. Since CMORPH estimates have pronounced error ( $-10 > \text{bias} (\%) > 10$ ), we first  
537 need to remove the bias before the product may be applied in hydrological and water resources  
538 applications. Figure 2 also show contours for rain gauge mean annual precipitation (MAP) in  
539 the Zambezi Basin with higher values in the northern parts of the basin (Kabompo and  
540 Luangwa) compared to the of lower localised estimates of MAP such as in Shire River and  
541 Kariba subbasins.

542

543



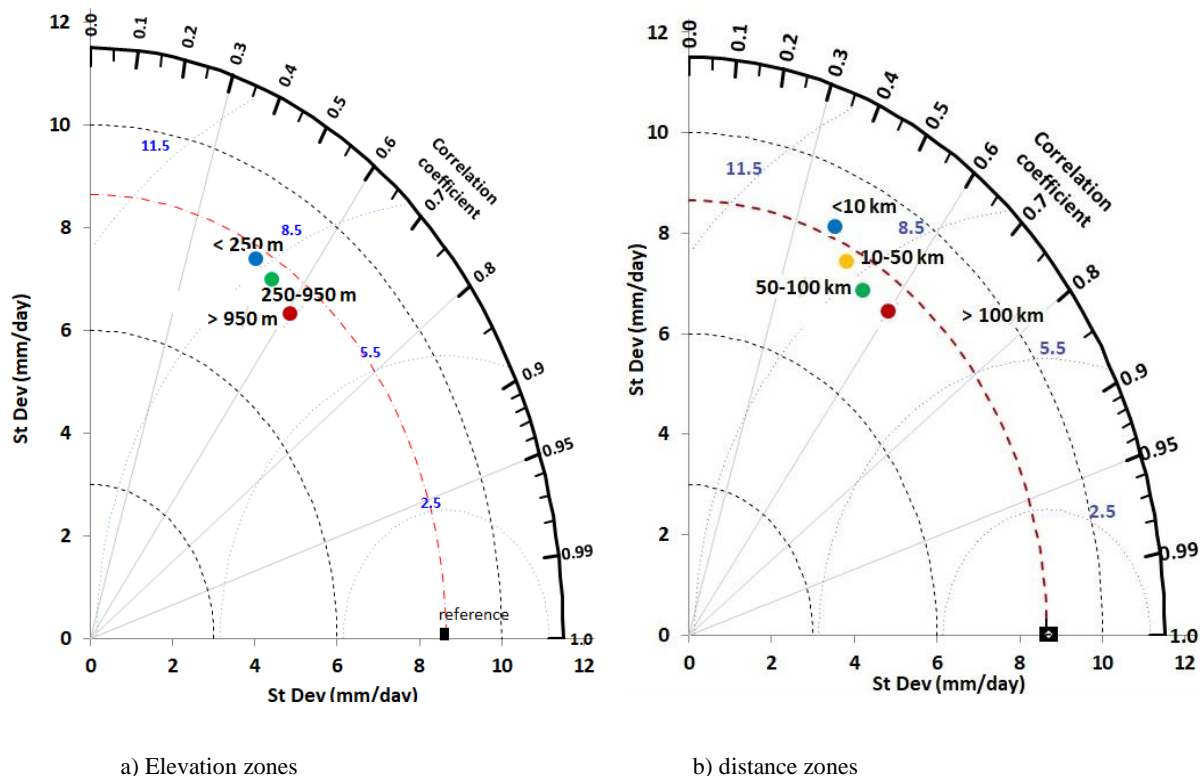
544  
 545 Figure 2: The spatial variation of bias (%) estimate for gauge vs CMORPH daily rainfall (1998-2013) for the Zambezi Basin.  
 546 The gauge based isohyets for Mean Annual Precipitation (MAP) are shown in blue.

547  
 548 **4.2. Effects of elevation and distance from large-scale open water bodies on CMORPH**  
 549 **bias**

551 Figure 3 shows Taylor diagrams with a comparison of basin lumped estimates of daily  
 552 uncorrected time series (1999–2013) of CMORPH and raingauge estimates for the 3 elevation  
 553 zones (left panes) and 4 distance zones from large-scale open water bodies (right panes). The  
 554 purpose of the diagrams is to show if elevation or distance from large-scale open water bodies  
 555 affect the performance in the CMORPH estimates. Here the performance in CMORPH is  
 556 defined for the root mean square difference ( $E$ ), correlation coefficient ( $R$ ) and standard  
 557 deviation. Figure 3 reveals that the standard deviations in the elevation zones and the distance  
 558 zones (except for the < 10 km distance zone) are lower than the reference/rain gauge standard  
 559 deviation which is indicated by the dashed brown arc (value of 8.45 mm/day). The stations in  
 560 the high elevation zone (> 950 m) and long distance zone (> 100 km) reveal lower variability  
 561 than stations at lower elevation and shorter distance zones. With respect to the reference line,  
 562 CMORPH estimates that are lumped for respective elevation zones and distance to a large  
 563 water body do not match standard deviation of raingauge based counterparts. Figure 3 also  
 564 reveals that CMORPH standard deviations that are close to gauge estimates belong to lower  
 565 elevation and shorter distance zones. Based on the Taylor diagrams, the statistics ( $R$  and  $E$ ) for  
 566 uncorrected CMORPH show increasing performance for increasing elevation and distance



567 from large-scale water bodies. Specifically, stations in the lower elevation zones (< 250m) have  
 568 lower  $R$  and higher  $E$  than the higher elevation zones (> 950 m). The shorter distance zones  
 569 also have lower  $R$  and higher  $E$  than for longer distance zones (> 100 km).  
 570



a) Elevation zones  
 b) distance zones

Figure 3. Time series of rain gauge (reference) vs CMORPH estimations, period 1999-2013, for elevation zones (left panes) and distance zones (right panes) in the Zambezi Basin. The correlation coefficients for the radial line denote the relationship between CMORPH and gauge based observations. Standard deviations on both the x and y axes show the amount of variance between the two-time series. The standard deviation of the CMORPH pattern is proportional to the radial distance from the origin. The angle between symbol and abscissa measures the correlation between CMORPH and rain gauge observations. The root mean square difference (blue contours) between the CMORPH and rain gauge patterns is proportional to the distance to the point on the x-axis identified as "reference". For details, see Taylor (2001)

571  
 572 Our results show that aspects of elevation and distance from large scale open water bodies are  
 573 distinctively represented (clear signature) in the relationship between CMORPH and gauge  
 574 rainfall in the Zambezi Basin. For elevation, Romilly and Gebremichael (2011) showed that  
 575 the accuracy of CMORPH at monthly time base is related to elevation for six river basins in  
 576 Ethiopia. A similar finding was reported by (e.g. Haile et al., 2009; Katiraie-Boroujerdy et al.,  
 577 2013; Rientjes et al., 2013a; Wu and Zhai, 2012) who found that performance of CMORPH is  
 578 affected by elevation. s. Contrary to these findings, Vernimmen et al. (2012) concluded that  
 579 TRMM Multi-satellite Precipitation Analysis (TMPA) 3B42RT performance was not affected  
 580 by elevation ( $R^2 = 0.0001$ ) for Jakarta, Bogor, Bandung, Java, Kalimantan and Sumatra regions  
 581 (Indonesia). The study by Gao and Liu (2013) showed that the bias in CMORPH rainfall over

582 the Tibetan Plateau is affected by elevation. Whilst distance from large scale open water bodies  
 583 and elevation have been assessed separately for this study, Habib et al. (2012a) revealed that  
 584 the two (distance from large scale open water bodies and elevation) interact in the Nile Basin  
 585 to produce unique circulation patterns to affect the performance of SRE.

586

587 We note that the overall performance could also be affected among other things by the sparse  
 588 and irregular distributed rain gauges in the Zambezi Basin.

589

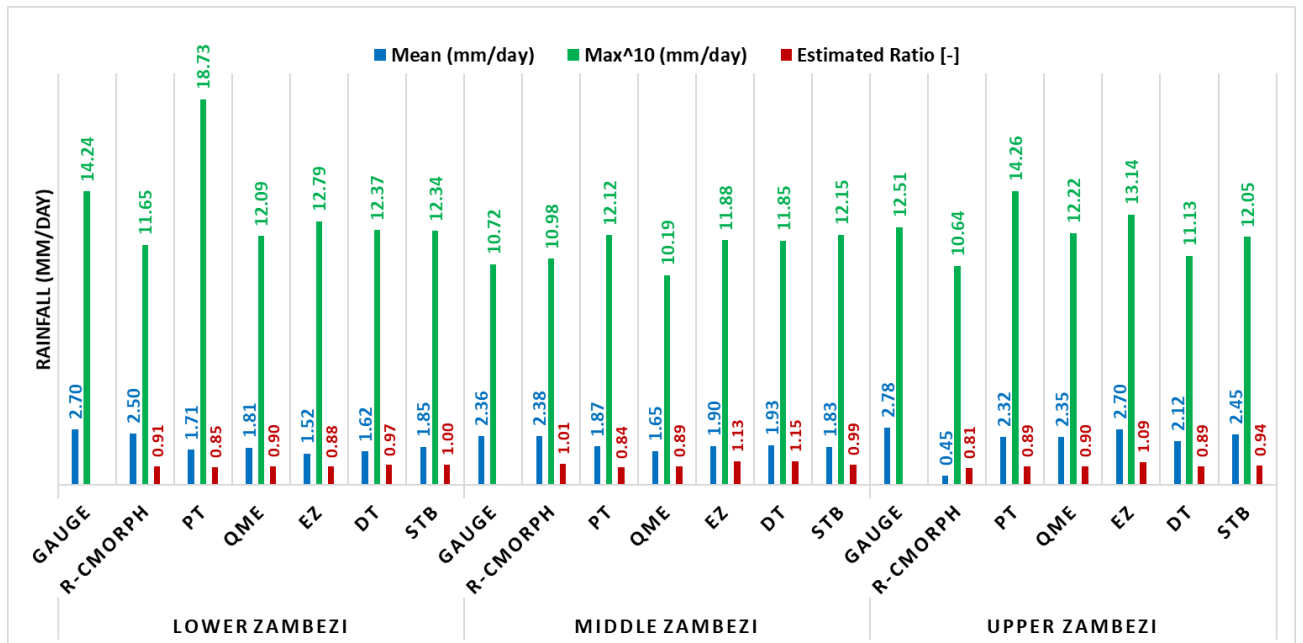
590 **4.3. Evaluation of bias correction**

591

592 **4.3.1. Standard statistics**

593 Figure 4 shows frequency based statistics (mean and maximum) on accuracy of CMORPH  
 594 rainfall estimates for each bias correction method. The ratio of cumulated estimates (1999-  
 595 2013) from gauged and CMORPH estimates for the Lower, Middle and Upper Zambezi  
 596 subbasins are shown. Results show that the bias of CMORPH moderately reduced for each of  
 597 the five bias correction schemes. However, the effectiveness of the schemes vary spatially with  
 598 best performance in Lower and Upper Zambezi subbasin and relatively poor performance in  
 599 the Middle Zambezi subbasin (see Figure 4).

600



601

602 Figure 4: Frequency based statistics (mean, max and estimated ratio of gauged sum vs CMORPH sum for 1999-2013) for the  
 603 Zambezi Basin.

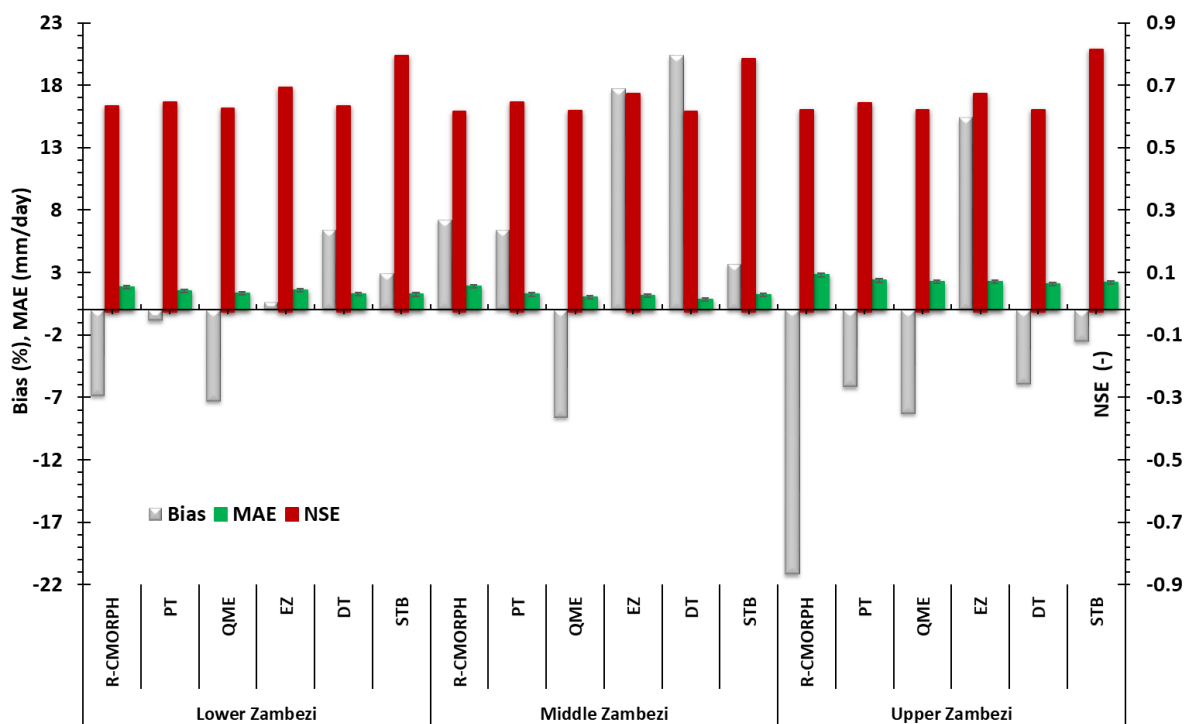
604

605 Judging by the three performance indicators (mean, max and estimated ratio), results indicate  
 606 that STB bias correction scheme is consistently effective in removing CMORPH rainfall bias  
 607 in the Zambezi Basin. STB and PT effectively adjust for the mean of CMORPH rainfall  
 608 estimates. Statistics in Figure 5 confirm these findings especially for the Upper Zambezi  
 609 subbasin where the mean of corrected estimates improved by > 60% from the mean of

610 uncorrected estimates. In addition, PT in the Lower Zambezi, QME in both Middle and Upper  
 611 Zambezi and STB in the Upper Zambezi were also effective (improvement by 16 %) in  
 612 correcting for the highest values in the rainfall estimates. STB performs better than other bias  
 613 schemes in reproducing rainfall for the Lower and Upper Zambezi subbasin, where the ratio of  
 614 gauge total to corrected CMORPH total is close to 1.0.

615  
 616 Figure 5 shows the mean absolute error (MAE) and percentage bias (% bias) on the left axis  
 617 and Nash Sutcliffe Efficiency (NSE) on the right axis. The three performance indicators were  
 618 used as a measure to evaluate performance of bias correction schemes in the Zambezi Basin.  
 619 The effectiveness of the bias correction by all schemes varies over the different parts of the  
 620 basin but is higher in Lower and Upper than in Middle Zambezi. The STB, PT and EZ shows  
 621 improved performance by exhibiting smaller MAEs compared to the uncorrected CMORPH  
 622 (R-CMORPH). A greater improvement is shown for the Middle Zambezi where the  
 623 uncorrected MAE of 1.89 mm/day is reduced to 0.86 mm/day after bias correction by the  
 624 elevation zone bias correction scheme (EZ). The signal on improved performance for the  
 625 Lower and Middle Zambezi as compared to the Upper Zambezi is also evident for the majority  
 626 of the bias correction techniques. However, relatively large error remains in the MAE.

627



628 Figure 5: Percentage bias, Mean Absolute Error (left axis) and Nash Sutcliffe (NSE) (right axis) of corrected and uncorrected  
 629 CMORPH (R-CMORPH) daily rainfall averaged for the Lower Zambezi, Middle Zambezi and Upper Zambezi.

630  
 631 The NSE for STB is above 0.8 for all three Zambezi subbasins. This is followed by EZ which  
 632 for all three subbasins s is above 0.7 for the three subbasins. The lowest NSE is for QME  
 633 which is close to 0.65 for all three subbasins. With regard to reducing bias (% bias), best results

634 are obtained by EZ in the Lower Zambezi (percentage bias of 0.7 % ~ absolute bias of 0.10  
635 mm/day) and Upper Zambezi (0.22 % ~0.23 mm/day), PT in the Lower and Middle Zambezi  
636 (-0.84 % ~0.18 mm/day) and STB in all the basins (< 3.70 % ~0.24 mm/day). Gao and Liu  
637 (2013) asserts that EZ (a correction process based on elevation) is valuable in correcting  
638 systematic biases to provide a more accurate precipitation input for rainfall-runoff modelling.  
639 Significant underestimation for the uncorrected (-21.16 % ~0.44 mm/day) and for bias  
640 corrected CMORPH are shown for the Upper Zambezi subbasin.

641

#### 642 4.3.2. Significance testing

643 Table 2 shows results of statistical tests to assess whether there is a significant difference ( $p <$   
644 0.05) between raingauge vs uncorrected and bias corrected CMORPH satellite rainfall for each  
645 of the 52 raingauge stations. Results are summarised for the Upper, Middle and Lower Zambezi  
646 and in the Zambezi basin. The null hypothesis is rejected for PT (Lower Zambezi), DT (Upper  
647 Zambezi) and QME (all the 3 sub-basins) since  $p < 0.05$ . This means that statistically the above  
648 mentioned bias correction schemes results deviate from the gauge. The null hypothesis is  
649 accepted for STB and EZ (all t three sub-basins), DT (Lower and Upper Zambezi) and PT  
650 (Middle and Upper Zambezi), since  $p > 0.05$  showing the effectiveness of these bias correction  
651 schemes. Compared to uncorrected satellite rainfall (R-MORPH), results also reveal that the  
652 bias corrected satellite rainfall is closer to the gauge based estimates.

653

654 Table 2: Paired t-tests for the Upper, Middle and Lower Zambezi. The mean difference is significant at the 0.05 level. Bold  
655 shows significant values..

Basin	Rainfall Estimate	t-value	Mean Std. Error	p-value (0.05)
Lower Zambezi	R-CMORPH	8.95	0.04	<b>0.04</b>
	DT	39.86	0.09	0.35
	PT	21.08	0.04	<b>0.03</b>
	QME	23.99	0.04	<b>0.04</b>
	EZ	36.43	0.03	0.27
	STB	14.7	0.04	0.46
Middle Zambezi	R-CMORPH	3.27	0.03	<b>0.001</b>
	DT	41.9	0.07	0.24
	PT	26.02	0.03	0.14
	QME	18.38	0.03	<b>0.00</b>
	EZ	26.60	0.02	0.07
	STB	23.6	0.03	0.09
Upper Zambezi	R-CMORPH	4.28	0.08	<b>0.00</b>
	DT	22.63	0.14	<b>0.01</b>
	PT	12.98	0.07	<b>0.05</b>
	QME	13.27	0.07	<b>0.00</b>
	EZ	13.73	0.07	0.14
	STB	13.62	<b>0.07</b>	<b>0.08</b>

656

657 **4.3.3. Analysis of variance (ANOVA test)**

658 The ANOVA test is similar to a t-test except that the test can be used to compare the means  
 659 from three or more data samples. Results of ANOVA shows that there is a significant ( $p < 0.05$ )  
 660 difference in the means of the 5 bias correction results across the three subbasins. This  
 661 warranted the running of a post-hoc test to determine which schemes differ significantly. The  
 662 contingency matrix in Table 2 shows results of the post-hoc tests results summarized for the  
 663 Tukey HSD, Scheffe and the Bonferroni methods but also for the Upper, Lower and Middle  
 664 Zambezi. Table 3 also show that STB, PT and EZ are significantly different from the  
 665 distribution transformation technique (DT) for the three sub-basins. STB, the best performing  
 666 bias correction scheme identified using majority of the indicators is also significantly different  
 667 from QME and EZ. QME which has poorly performed is significantly different from EZ.  
 668 Results are important for further application of the bias correction schemes for studies such as  
 669 flood, drought and water resources modelling.

670  
 671 Table 3: ANOVA post-hoc tests for the results of the five bias correction schemes ( $p < 0.05$ ). The checklist table gives a  
 672 indication (symbol) where two bias correction scheme's results are significantly different from each other. Where there is no  
 673 symbol, it means that the schemes' results are not significantly different. The different symbols represent the Upper, Middle  
 674 and Lower Zambezi basins.  
 675

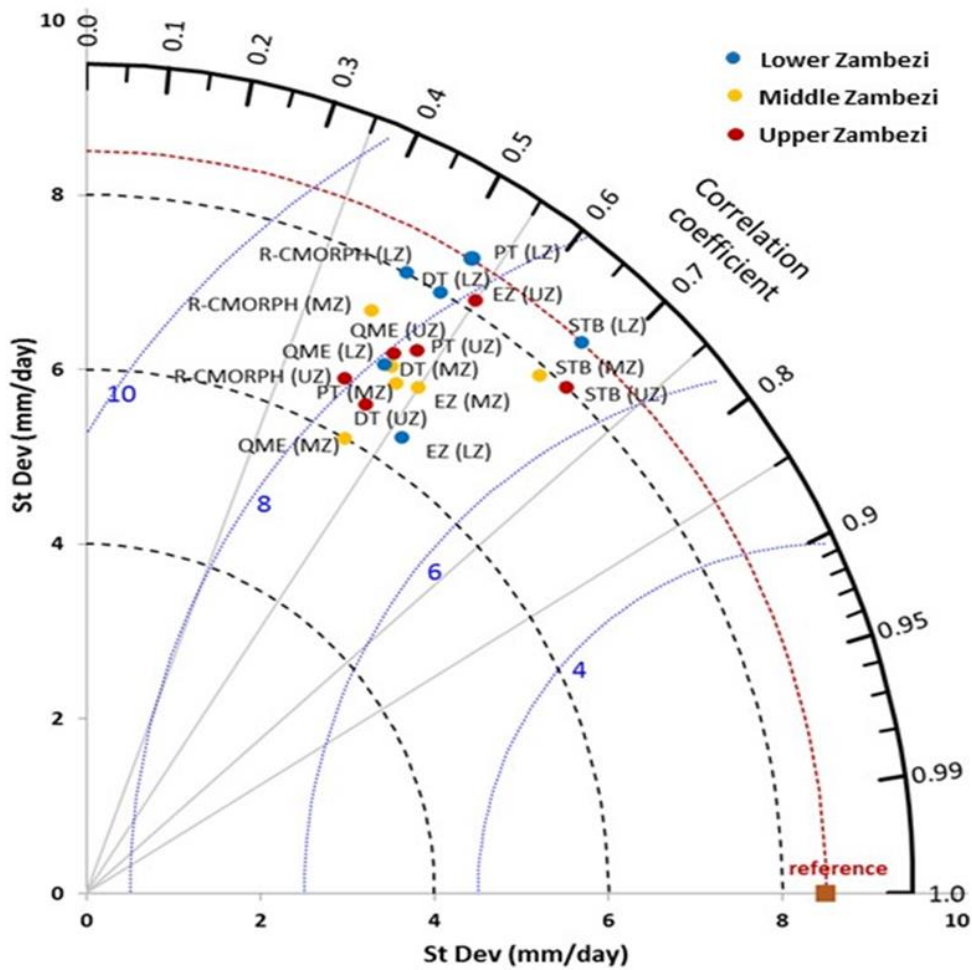
	STB	PT	QME	DT	EZ
STB			✓	✗ ✓	✓
PT			✓	✗ ✓	
QME	✓				✓
DT	✗ ✓	✗ ✓	✗ ✓		✗ ✓
EZ	✓			✗ ✓	
<b>Key</b>		✗	Upper Zambezi		
		✓	Lower Zambezi		
		✓	Middle Zambezi		

676  
 677  
 678 **4.3.4. Taylor Diagrams**  
 679

680 Figure 6 shows the Taylor diagram for time series of rain gauge (reference) observations vs  
 681 CMORPH bias correction schemes averaged for the Lower Zambezi (UZ), Middle Zambezi  
 682 (MZ) and Upper Zambezi (UZ). Absolute values used to develop the Taylor diagram are shown  
 683 in Appendix 2. The position of each bias correction scheme and uncorrected satellite rainfall  
 684 (R-MORPH) on Figure 6 shows how closely the rainfall by R-MORPH matches rain gauge  
 685 observations as well as effectiveness of each of the bias schemes. Overall, all bias correction  
 686 schemes show intermediate performance in terms of bias removal. Only the PT and STB for  
 687 the Lower Zambezi subbasin lie on the line of standard deviation (brown dashed arc) and means  
 688 the standard deviation of the data for the two bias correction schemes matches the gauge  
 689 observations. This also indicates that rainfall variations after PT and STB bias correction for  
 690 the Lower Zambezi resembles gauge based standard deviation. Note however that STB  
 691 performs better than EZ as shown by the superior correlation coefficient. Compared against the  
 692 reference line of mean standard deviation (8.5 mm/day), the rainfall standard deviation for most  
 693 bias correction schemes is below this line and as such exhibit low variability across the  
 694 Zambezi Basin.

695  
 696  
 697  
 698  
 699  
 700  
 701  
 702  
 703  
 704  
 705

Figure 6 also shows that most of the bias correction schemes have standard deviation range of 6.0 to 8.0 mm/day. There is a consistent pattern between the bias correction schemes that have low R and high RMSE difference indicating that these schemes are not effective in bias removal. Overall, the best performing bias correction schemes (STB and EZ) have  $R > 0.6$ , standard deviation relatively close to the reference point and  $RMSE < 7$  mm/day. The uncorrected CMORPH (R-MORPH) lies far away from the marked reference (gauge) point on the x-axis suggesting an intermediate overall effectiveness of the bias correction schemes such as STB, EZ, DT and PT in removing error as they are relatively closer to the marked reference point.



706  
 707  
 708  
 709  
 710  
 711  
 712

Figure 6: Taylor's diagram on Rain gauge (reference) observations and CMORPH bias corrected estimates (all 5 schemes) as averaged for the Lower Zambezi (LZ), Middle Zambezi (MZ), and Upper Zambezi (UZ) for the period 1999-2013. The distance of the symbol from point (1, 0) is also a relative measure of the bias correction scheme performance. The position of each symbol appearing on the plot quantifies how closely precipitation estimates by respective bias correction scheme's matches counterparts by rain gauge. The dashed blue lines indicate the root mean square difference (mm/day).

713  
 714  
 715  
 716

The least performing bias correction scheme is QME relatively large RSMD ( $> 8$  mm/day) and with low  $R$  ( $< 0.49$ ) and standard deviation ( $< 6.5$  mm/day). Inherent to the methodology of most of bias correction schemes (e.g. QME) is that the spatial pattern of the SRE does not change and therefore the  $R$  for a specific station for daily precipitation does not necessarily



717 improve. The bias correction results by the Taylor Diagram in Figure 6 corroborates with  
 718 findings shown in Figure 4 and Figure 5 for mean, max, ratio of rainfall totals and bias as  
 719 performance indicators.

720  
 721

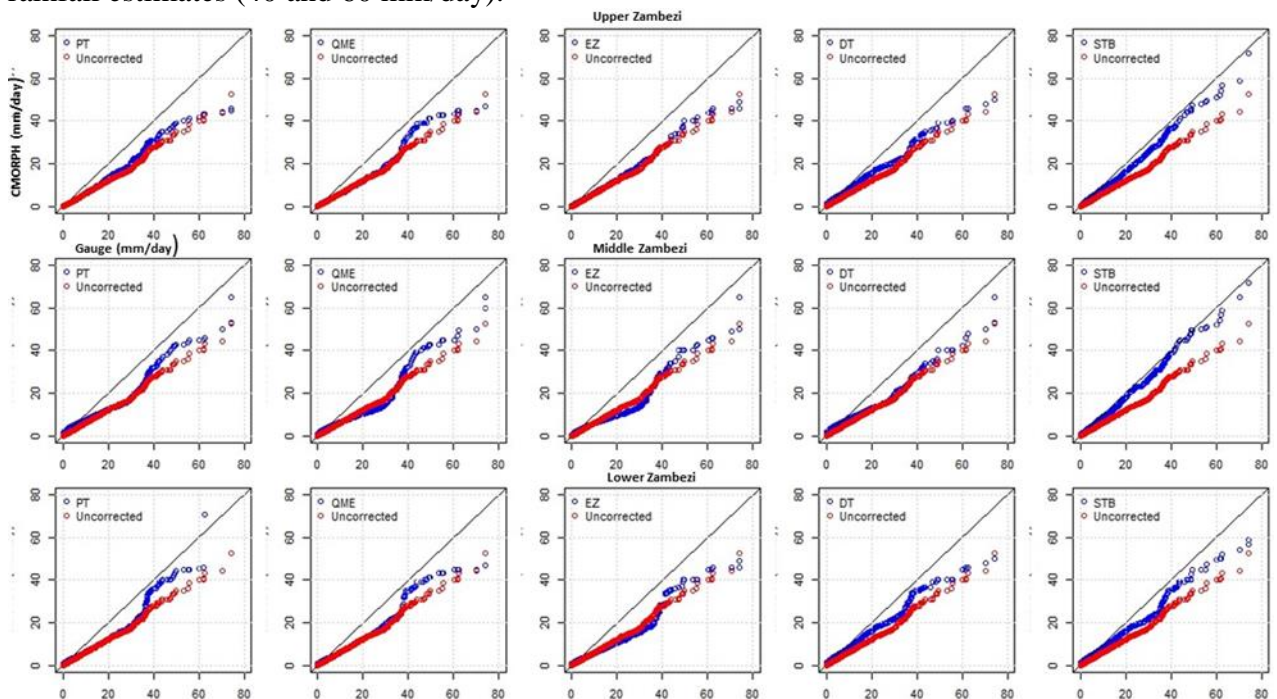
722 **4.3.5. q-q plots**

723

724 Figure 7 shows q-q plots for the Upper, Middle and Lower Zambezi for gauge estimates against  
 725 uncorrected and bias corrected CMORPH rainfall. Results show that the STB q-q plots for bias  
 726 corrected CMORPH across the 3 basins has majority of points that fall approximately along  
 727 the 45-degree reference line. This means that the STB bias corrected satellite rainfall has closer  
 728 distribution to the raingauge as compared to the uncorrected CMORPH counterparts suggesting  
 729 effectiveness of the bias correction scheme. Other bias correction schemes such as QME, EZ  
 730 and PT have data points showing a greater departure from the 45-degree reference line so  
 731 performance is less effective.

732

733 In some instances in both the Upper, Middle and Lower Zambezi, bias corrected values are  
 734 significantly higher than the corresponding gauge values whereas in some instances there is  
 735 serious underestimation. All tq-q plots also show that for all bias correction schemes, the  
 736 differences between gauge and satellite rainfall are minimal for low rainfall rates (< 2.5  
 737 mm/day) and increasing for heavy rainfall (> 20.0 mm/day). In more detail, all the bias  
 738 correction schemes show a larger difference for the transition area from low to heavy rainfall.  
 739 QME and PT are not in good agreement with the rest of the bias correction schemes for higher  
 740 rainfall estimates (40 and 60 mm/day).

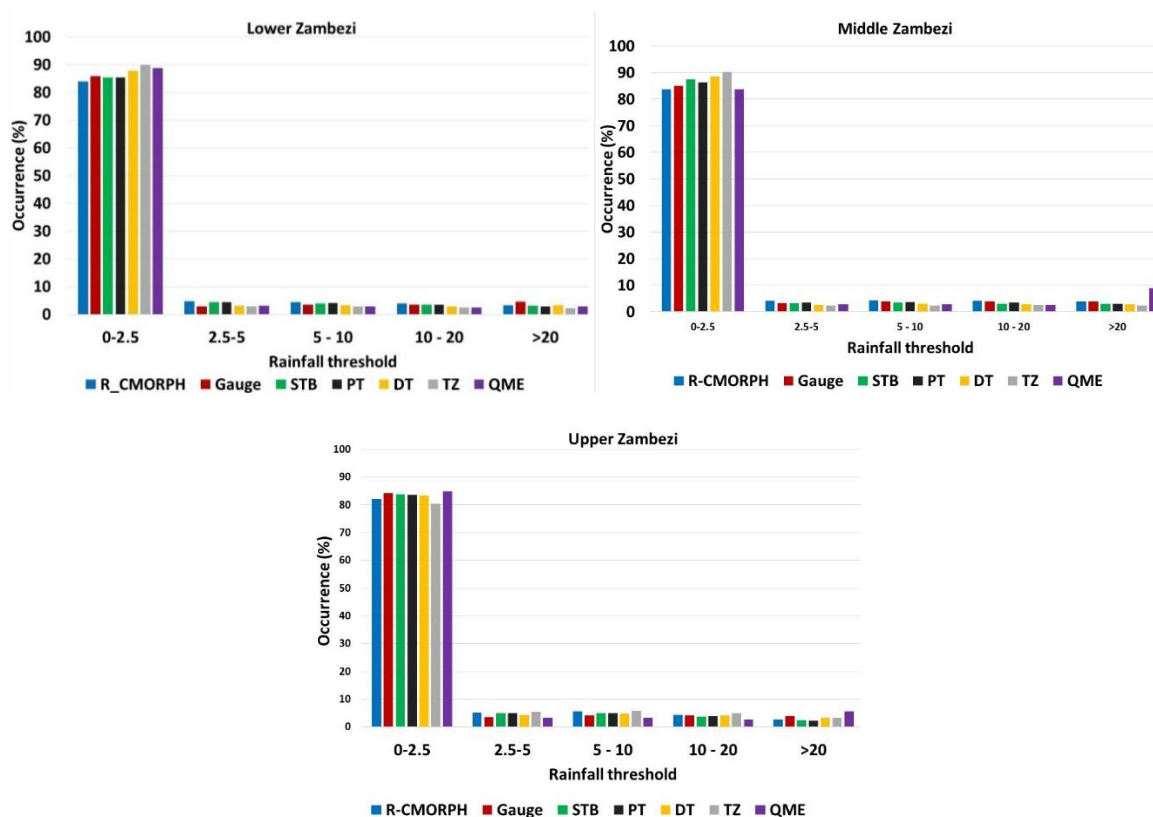


741  
 742 Figure 7: q-q plot for gauge vs satellite rainfall (corrected and bias corrected) for the Upper (top panes),  
 743 Middle (middle panes) and Lower (bottom panes) Zambezi.  
 744

745  
 746  
 747  
 748  
 749  
 750  
 751  
 752  
 753  
 754  
 755  
 756  
 757  
 758  
 759  
 760  
 761  
 762

### 4.3.6. CMORPH rainy days

Occurance (%) of rainfall rates in the Zambezi Basin for each bias correction scheme is shown in Figure 8. The highest percentage (80-90 %) is shown for very light rainfall (0.0-2.5 mm/day). A smaller percentage is shown for 2.5-5.0 mm/day which is the light rainfall class. Smallest percentage (< 5%) is shown for heavy rainfall (> 20.0 mm/day). The CMORPH rainfall corrected with STB, PT and DT matches the gauge based rainfall (%) in the Lower, Middle and Upper Zambezi suggesting good performance. All five bias correction schemes in the Zambezi Basin generally tend to overestimate low rainfall (< 2.5 mm/day). There is a small difference for moderate rainy days classification of 10.0-20.0 mm/day. For QME in the Middle and Upper Zambezi, there is overestimation by > 80 %. There is underestimation of rainfall greater than 20 mm/day. Results are consistent with findings by Gao and Liu (2013) in the Tibetan Plateau who also found consistent under and overestimation of occurrence by CMORPH for rainfall rates >10.0 mm/day. A study by Zulkafli et al. (2014) in French Guiana and North Brazil noted that the low sampling frequency and consequently missed short-duration precipitation events between satellite measurements results in underestimation, particularly for heavy rainfall.



763  
 764

Figure 8: Percentage occurrence for rainfall rate classes

765  
 766  
 767  
 768  
 769  
 770

Figure 9 gives the bias correction performance for the different rainy day classes. Results of bias removal varies for the Lower, Middle and Upper Zambezi. Comparatively, the STB and EZ show effectiveness in bias removal with an average bias correction of 0.97 % and 3.6 % in



771 the whole basin respectively. Results show more effectiveness in reducing the percentage bias  
 772 for light rainfall and moderate rainfall (0-2.5 and 5.0-10.0 mm/day) than the high to very high  
 773 rainfall (10.0-20.0 mm/day and >20.0 mm/day) across the whole basin. The poor performance  
 774 of correction for the heavy rainfall class is caused by, sometimes, large mismatch of high rain  
 775 gauge values versus low CMORPH values. This leads to unrealistically high CMORPH values  
 776 which remain poorly corrected by bias schemes.  
 777



778  
 779 Figure 9: Bias correction (%) for respective rainfall rate classes  
 780

781 **4.4. Spatial cross-validation**

782 Table 4 shows the cross-validation results on bias correction for 8 stations for wet and dry  
 783 seasons. It is evident that CMORPH has a considerable bias, although this bias is not always  
 784 consistent for all 8 validation stations. Overall, Mutarara station has the highest positive bias  
 785 (overestimation) whereas Makhanga has the highest negative bias (underestimation) for  
 786 uncorrected CMORPH. Bias is effectively being removed by the STB followed by the EZ bias  
 787 correction schemes. Bias is more effectively removed for the wet season than for the dry  
 788 season. For the dry season, the STB shows good performance for Mkhanga and Nchalo stations,  
 789 whereas good performance is shown for Kabompo and Chichiri stations. However, the MAE  
 790 is higher for the wet season than for the dry season. Correlation coefficient for bias corrected  
 791 satellite rainfall is higher for the wet season than for the dry season. The study by Ines and  
 792 Hansen (2006) for semi-arid eastern Kenya showed that multiplicative bias correction schemes  
 793 such as STB were effective in correcting the total of the daily rainfall grouped into seasons.  
 794 Our results show that effectiveness in bias removal in the wet season is higher than in the dry  
 795 season This is contrary to Vernimmen et al. (2012) who showed that for the dry season, bias

796 for PT decreased in Jakarta, Bogor, Bandung, East Java and Lampung regions after bias  
 797 correction of monthly TMPA 3B42RT precipitation estimates over the period 2003–2008.  
 798 Habib (2014) evaluated sensitivity of STB for the dry and wet season and concluded that the  
 799 bias correction factor for CMOPRH shows lower sensitivity for the wet season as compared to  
 800 the dry season. Our findings also reveal that bias factors for all the schemes are more variable  
 801 in the dry season than in the wet season and lead to poor performance of the bias correction  
 802 schemes in the dry season.

803  
 804 Validation results for all 8 stations for the period 1999-2013 show that the bias on CMORPH  
 805 reduces the MAE by 23 %. This represents 22 % of the average MAE estimated using 52  
 806 raingauges. Since the stations used for validation are different from the stations used to develop  
 807 the bias correction procedures, we conclude that the results are independent of deliberate efforts  
 808 to reducing the errors. Similar cross-validation techniques where measures of performance are  
 809 evaluated using a sample that was not included in the calibration of the correction procedure  
 810 gave good performance in the the state of Rhineland-Palatinate in Europe (Gutjahr and  
 811 Heinemann, 2013).

812  
 813 Table 4: Cross validation results for the bias correction procedure with 8 gauging stations for the dry and wet season. Stations  
 814 lie at average elevation zone and sort of centred in an elevation zone. R-Morph is the uncorrected R-CMOPRH estimate. DT,  
 815 PT, QME, EZ and STB are the bias corrected rainfall estimate. Bold values indicate best performance. \* = zone 1: elevation  
 816 of < 250 m , \*\* = zone 2: elevation range of 250 - 950 m and \*\*\* = zone 3: elevation > 950 m

Station	Rainfall Estimate	Dry Season (April-Sept)				Wet Season (Oct-March)			
		Bias (%)	MAE	Correlation	Estimated Ratio	Bias (%)	MAE	Correlation	Estimated Ratio
Makhanga*	R-CMORPH	-28.69	1.23	0.42	0.87	-21.17	8.63	0.43	0.91
	DT	-1.37	0.53	0.56	0.99	-1.66	3.96	0.65	0.94
	PT	-5.62	0.52	0.54	0.95	-3.5	4.67	0.64	1.02
	QME	1.98	0.54	0.54	0.95	-0.64	4.86	0.65	0.97
	EZ	2.10	0.47	0.55	1.03	-0.11	4.08	0.58	0.96
	STB	0.77	0.61	0.56	1.04	0.5	5.06	0.62	1.02
Nchalo*	R-CMORPH	-33.05	1.13	0.42	0.84	-25.18	8.05	0.38	0.83
	DT	-0.23	0.73	0.56	0.96	-2.61	3.65	0.50	0.87
	PT	-4.28	0.68	0.54	0.93	-6.48	5.05	0.59	0.92
	QME	1.90	0.72	0.53	0.81	-0.56	5.29	0.53	0.91
	EZ	0.35	0.63	0.54	0.99	<b>0.22</b>	4.4	0.60	1.06
	STB	-0.43	0.73	0.58	0.96	-1.23	5.54	0.61	1.02
Rukomichi**	R-CMORPH	-23.05	0.93	0.42	0.86	-21.18	6.69	0.31	0.73
	DT	-0.23	0.90	0.56	0.94	-6.2	3.51	0.60	0.87
	PT	-4.28	0.73	0.54	0.93	-2.48	3.62	0.59	0.92
	QME	1.90	0.75	0.53	1.03	-0.56	3.88	0.54	0.83
	EZ	0.35	0.71	0.54	0.99	<b>0.22</b>	3.5	0.60	1.06
	STB	-0.43	0.76	0.58	0.94	-1.26	3.33	0.61	1.02
Mutarara**	R-CMORPH	20.15	0.24	0.49	1.10	20.1	2.34	0.50	1.05
	DT	11.4	0.18	0.60	1.03	8.7	1.23	0.63	1.04
	PT	8.4	0.12	0.55	0.91	4.3	1.28	0.68	1.03
	QME	5.7	0.14	0.63	1.1	8.1	1.4	0.65	0.98

	EZ	-12.8	<b>0.09</b>	0.54	0.95	1.9	1.23	0.69	1.03
	STB	4.5	0.14	0.53	1.1	2.1	1.33	<b>0.73</b>	<b>1.01</b>
Mfuwe**	R-CMORPH	40.2	0.28	0.45	0.85	35.4	6.4	0.48	1.08
	DT	2.9	0.62	0.53	0.96	4.6	3.9	0.62	0.98
	PT	3.7	0.22	0.55	0.92	7.9	5.25	0.65	0.96
	QME	3.9	0.30	0.55	0.93	5.4	5.68	0.64	0.97
	EZ	6.1	0.24	0.54	0.92	3.8	5.18	0.56	0.98
	STB	5.4	0.26	0.65	0.93	1.2	4.66	0.65	0.96
Kabombo***	R-CMORPH	25.3	0.70	0.44	0.95	24.3	3.8	0.48	0.85
	DT	7.7	0.32	0.51	0.96	5.7	3.5	0.62	0.94
	PT	9.2	0.13	0.54	1.10	8.7	3.0	0.64	0.96
	QME	2.7	0.32	0.62	1.10	2.8	3.2	0.63	0.95
	EZ	5.6	0.22	0.53	0.91	3.3	2.7	0.54	0.96
	STB	19	0.13	0.62	1.01	9.3	2.7	0.64	0.93
Chichiri***	R-CMORPH	34.5	1.56	0.47	0.8	-37.3	4.7	0.45	0.84
	DT	12.2	0.60	0.51	0.85	5.5	3.2	0.51	0.93
	PT	9.4	0.42	0.52	1.04	-7.8	4.1	0.54	0.95
	QME	8.4	0.92	0.56	1.05	-13.0	4.1	0.64	1.04
	EZ	-13	0.61	0.60	0.94	-9.9	4.2	0.60	0.96
	STB	3.2	0.45	0.63	0.98	-14.3	2.1	0.65	<b>0.99</b>
Chitedze***	R-CMORPH	41.5	0.90	0.47	1.06	42.3	5.4	0.48	0.89
	DT	16.7	0.53	0.54	0.98	-13.2	3.3	0.62	0.86
	PT	-16.5	0.44	0.55	0.99	22.2	4.5	0.65	1.05
	QME	18.2	0.41	0.57	1.04	18.5	4.3	0.64	1.04
	EZ	11.7	0.32	0.57	1.02	8.4	4.6	0.55	1.03
	STB	3.9	0.23	0.60	0.03	-8.2	3.7	0.65	0.97

817

#### 818 **4.5. Temporal cross-validation**

819 The same performance indicators in spatial cross-validation are calculated for the temporal  
820 cross-validation. Results are presented in Table 5. The structure of the error is the same as in  
821 Table 4, where the MAE is higher for the wet season than for the dry season. However,  
822 compared to the spatial cross-validation the difference in effectiveness in the error removal  
823 between the dry and wet season is much larger due to the limited length of the time series  
824 (1998-1999). STB outperforms both bias correction methods but does also have problems  
825 correcting the estimated ratios. After the correction, the correlation coefficient is much  
826 improved. The fact that MAE remains relatively large indicates that errors remain  
827 locally large. These values are almost in same range to performance indicators obtained from  
828 the main performance assessment period (1999-2013). However using one year (1998-1999)  
829 to correct bias in CMORPH increased the MAE by 10 % compared to the main performance  
830 assessment period (1999-2013) The estimated ratio adjustment in the temporal cross-validation  
831 reduced by 7 % from the 1999-2013 period.

832

833

834

835

Table 5: Temporal-cross validation results for the period 1998-1999 for the wet and dry season

Station	Rainfall Estimate	Dry Season (April-Sept)				Wet Season (Oct-March)			
		Bias (%)	MAE	Correlation	Estimated Ratio	Bias (%)	MAE	Correlation	Estimated Ratio
Lower Zambezi	R-CMORPH	-28.26	1.10	0.42	0.86	-22.51	7.79	0.37	0.82
	DT	-0.61	0.72	0.56	0.96	-3.49	3.71	0.58	0.89
	PT	-4.73	0.64	0.54	0.94	-4.15	4.45	0.61	0.95
	QME	1.93	0.67	0.53	0.93	-0.59	4.68	0.57	0.90
	EZ	0.93	0.60	0.54	1.00	0.11	3.99	0.59	1.03
	STB	-0.03	0.70	0.57	0.98	-0.66	4.64	0.61	1.02
Middle Zambezi	R-CMORPH	28.55	0.41	0.46	0.97	26.60	4.18	0.49	0.99
	DT	7.33	0.37	0.55	0.98	6.33	2.88	0.62	0.99
	PT	7.10	0.16	0.55	0.98	6.97	3.18	0.66	0.98
	QME	4.10	0.25	0.60	1.04	5.43	3.43	0.64	0.97
	EZ	-0.37	0.18	0.54	0.93	3.00	3.04	0.60	0.99
	STB	9.63	0.18	0.60	1.01	4.20	2.90	0.67	0.97
Upper Zambezi	R-CMORPH	38	1.23	0.47	0.93	2.5	5.05	0.465	0.865
	DT	14.45	0.565	0.525	0.915	-3.85	3.25	0.565	0.895
	PT	-3.55	0.43	0.535	1.015	7.2	4.3	0.595	1
	QME	13.3	0.665	0.565	1.045	2.75	4.2	0.64	1.04
	EZ	-0.65	0.465	0.585	0.98	-0.75	4.4	0.575	0.995
	STB	3.55	0.34	0.615	0.505	-11.25	2.9	0.65	0.98

837

838 **5. Conclusions**

839 We present methods to assess the performance of bias correction schemes for CMORPH  
840 rainfall estimates in the Zambezi River Basin. Conclusions of this study are:

841 1. Analysis on gauge and CMORPH rainfall estimates shows that performance increases for  
842 higher elevation (>950 m) in the Zambezi Basin and that CMORPH has largest mismatch  
843 at low elevation. Such analysis was established for rain gauges within elevation classes of  
844 < 250 m, 250 - 950 m and > 950 m. The match between gauge and CMORPH estimates  
845 improved at increasing distance to large-scale open water bodies (poorest for short  
846 distances). This was established for rain gauges located within specified distances of < 10  
847 km, 10 -50 km, 50 -100 km and > 100 km to a large scale open water body.

848

849 2. For each of the five bias correction methods applied, accuracy of the CMORPH satellite  
850 rainfall estimates improved. Assessment through standard statistics, Taylor Diagrams, t-  
851 tests, ANOVA and q-q plots reveal that STB that accounts space and time variation of bias,  
852 is found more effective in reducing rainfall bias in the basin than the rest of the bias  
853 correction schemes. This indicates that the temporal aspect of CMORPH bias is more  
854 important than the spatial aspect in the Zambezi Basin. Quantile-quantile (q-q) plots for all  
855 the bias correction schemes show, in general, that bias corrected rainfall is in good  
856 agreement with gauge based estimates for low rainfall rates but that high rainfall rates are  
857 largely overestimated.

858

859 3. Evaluation of results by the five bias correction schemes was successfully performed using  
860 spatial and temporal cross-validation. The hold-out sample of 8 stations in this work  
861 showed the applicability of different bias correction methods under different geographical  
862 space (spatial). It is noted that the relatively short time series used for temporal validation  
863 may have affected results.

864

865 4. Differences in the mechanisms that drive precipitation throughout the year could result in  
866 different biases for each of the seasons, which motivated us to calculate the bias correction  
867 factors for each of the seasons separately. CMORPH rainfall time series were divided into  
868 wet and dry seasonal periods to assess the influence of seasonality on performance of bias  
869 correction schemes. Overall, the bias correction schemes reveal that bias removal is more  
870 effective in the wet season than in the dry season.

871

872 5. We assessed whether bias correction varies for different rainfall rates of daily rainfall in  
873 the Zambezi Basin. There is overestimation of very light rainfall (< 2.5 mm/day) and  
874 underestimation of very heavy rainfall (>20 mm/day) after application of the bias correction  
875 schemes. Bias was more effectively reduced for very low to moderate rainfall (< 2.5 and  
876 5.0-10.0 mm/day) than for high to very high rainfall (10.0-20.0 mm/day and >20.0  
877 mm/day). Overall, the STB and EZ more consistently removed bias in all the rainy days  
878 classification compared to the three other bias correction schemes.

879

880 Analysis serve to improve reliability of SREs applications in water resource applications in the  
881 Zambezi basin such as in drought analysis, flood prediction, weather forecasting and rainfall  
882 runoff modelling. In follow-up studies, we aim at hydrologic evaluation of bias corrected  
883 CMORPH rainfall estimates at the headwater catchment of the Zambezi River.

884

#### 885 **Acknowledgements**

886 The study was supported by WaterNet through the DANIDA Transboundary PhD Research in  
887 the Zambezi Basin and the University of Twente's ITC Faculty. The authors acknowledge the  
888 University of Zimbabwe's Civil Engineering Department for platform to carry out this  
889 research.

890

#### 891 **Author Contributions**

892 Webster Gumindoga was responsible for the development of bias correction schemes in the  
893 Zambezi basin and research approach. Tom Rientjes and Alemseged Haile were responsible  
894 for synthesising the methodology and made large contributions to the manuscript write-up.  
895 Hodson Makurira provided some of the rain gauge data and related findings of this study to

896 previous work in the Zambezi Basin. Reggiani Paulo assisted in interpretation of bias  
897 correction results.

898

899

## 900 **Conflict of Interests**

901

902 The authors declare no conflict of interests.

903

## 904 **References**

905 Beilfuss, R., Dutton, P., and Moore, D.: Landcover and Landuse change in the Zambezi Delta,  
906 in: Zambezi Basin Wetlands Volume III Landuse Change and Human impacts, Chapter  
907 2, Biodiversity Foundation for Africa, Harare, 31-105, 2000.

908 Beilfuss, R.: A Risky Climate for Southern African Hydro: Assessing hydrological risks and  
909 consequences for Zambezi River Basin dams, 2012.

910 Beyer, M., Wallner, M., Bahlmann, L., Thiemig, V., Dietrich, J., and Billib, M.: Rainfall  
911 characteristics and their implications for rain-fed agriculture: a case study in the Upper  
912 Zambezi River Basin, *Hydrological Sciences Journal*, null-null,  
913 10.1080/02626667.2014.983519, 2014.

914 Bitew, M. M., and Gebremichael, M.: Evaluation of satellite rainfall products through  
915 hydrologic simulation in a fully distributed hydrologic model, *Water Resources*  
916 *Research*, 47, 2011.

917 Bitew, M. M., Gebremichael, M., Ghebremichael, L. T., and Bayissa, Y. A.: Evaluation of  
918 High-Resolution Satellite Rainfall Products through Streamflow Simulation in a  
919 Hydrological Modeling of a Small Mountainous Watershed in Ethiopia, *Journal of*  
920 *Hydrometeorology*, 13, 338-350, 10.1175/2011jhm1292.1, 2011.

921 Bouwer, L. M., Aerts, J. C. J. H., Van de Coterlet, G. M., Van de Giessen, N., Gieske, A., and  
922 Manaerts, C.: Evaluating downscaling methods for preparing Global Circulation Model  
923 (GCM) data for hydrological impact modelling. Chapter 2, in Aerts, J.C.J.H. &  
924 Droogers, P.

925 Brown, A. M.: A new software for carrying out one-way ANOVA post hoc tests, *Comput.*  
926 *Methods Programs Biomed.*, 79(1), 89–95,  
927 doi:<https://doi.org/10.1016/j.cmpb.2005.02.007>, 2005.

928 (Eds.), *Climate Change in Contrasting River Basins: Adaptation Strategies for Water, Food*  
929 *and Environment*. (pp. 25-47). Wallingford, UK: Cabi Press., 2004.

930 Cecinati, F., Rico-Ramirez, M. A., Heuvelink, G. B. M., and Han, D.: Representing radar  
931 rainfall uncertainty with ensembles based on a time-variant geostatistical error  
932 modelling approach, *Journal of Hydrology*, 548, 391-405,  
933 <http://dx.doi.org/10.1016/j.jhydrol.2017.02.053>, 2017.

934 Cohen Liechti, T., Matos, J. P., Boillat, J. L., and Schleiss, A. J.: Comparison and evaluation  
935 of satellite derived precipitation products for hydrological modeling of the Zambezi  
936 River Basin, *Hydrol. Earth Syst. Sci.*, 16, 489-500, 2012.

937 Cuvelier, C., Thunis, P., Vautard, R., Amann, M., Bessagnet, B., Bedogni, M., Berkowicz, R.,  
938 Brandt, J., Brocheton, F., Builtjes, P., Carnavale, C., Coppalle, A., Denby, B., Douros,  
939 J., Graf, A., Hellmuth, O., Hodzic, A., Honoré, C., Jonson, J., Kerschbaumer, A., de  
940 Leeuw, F., Minguzzi, E., Moussiopoulos, N., Pertot, C., Peuch, V. H., Pirovano, G.,  
941 Rouil, L., Sauter, F., Schaap, M., Stern, R., Tarrason, L., Vignati, E., Volta, M., White,  
942 L., Wind, P., and Zuber, A.: CityDelta: A model intercomparison study to explore the

943 impact of emission reductions in European cities in 2010, *Atmospheric Environment*,  
944 41, 189-207, <http://dx.doi.org/10.1016/j.atmosenv.2006.07.036>, 2007.

945 Dennis, R., Fox, T., Fuentes, M., Gilliland, A., Hanna, S., Hogrefe, C., Irwin, J., Rao, S. T.,  
946 Scheffe, R., Schere, K., Steyn, D., and Venkatram, A.: A framework for evaluating  
947 regional-scale numerical photochemical modeling systems, *Environmental Fluid*  
948 *Mechanics*, 10, 471-489, 10.1007/s10652-009-9163-2, 2010.

949 Dinku, T., Chidzambwa, S., Ceccato, P., Connor, S. J., and Ropelewski, C. F.: Validation of  
950 high-resolution satellite rainfall products over complex terrain, *International Journal of*  
951 *Remote Sensing*, 29, 4097-4110, 10.1080/01431160701772526, 2008.

952 Fang, G. H., Yang, J., Chen, Y. N., and Zammit, C.: Comparing bias correction methods in  
953 downscaling meteorological variables for a hydrologic impact study in an arid area in  
954 China, *Hydrol. Earth Syst. Sci.*, 19, 2547-2559, 10.5194/hess-19-2547-2015, 2015.

955 Field, A.: *Discovering statistics using SPSS 2nd ed.* Sage Publications, 2009.

956 Fylstra, D., Lasdon, L., Watson, J., and Waren, A.: Design and Use of the Microsoft Excel  
957 Solver, *Interfaces*, 28, 29-55, doi:10.1287/inte.28.5.29, 1998.

958 Gao, Y. C., and Liu, M. F.: Evaluation of high-resolution satellite precipitation products using  
959 rain gauge observations over the Tibetan Plateau, *Hydrol. Earth Syst. Sci.*, 17, 837-849,  
960 10.5194/hess-17-837-2013, 2013.

961 Gebregiorgis, A. S., Tian, Y., Peters-Lidard, C. D., and Hossain, F.: Tracing hydrologic model  
962 simulation error as a function of satellite rainfall estimation bias components and land  
963 use and land cover conditions, *Water Resources Research*, 48, n/a-n/a,  
964 10.1029/2011wr011643, 2012.

965 Grillakis, M. G., Koutroulis, A. G., Daliakopoulos, I. N., and Tsanis, I. K.: A method to  
966 preserve trends in quantile mapping bias correction of climate modeled temperature,  
967 *Earth Syst. Dynam. Discuss.*, 2017, 1-26, 10.5194/esd-2017-53, 2017.

968 Gutjahr, O. and Heinemann, G.: Comparing precipitation bias correction methods for high-  
969 resolution regional climate simulations using COSMO-CLM, *Theor. Appl. Climatol.*,  
970 114(3-4), 511-529, doi:10.1007/s00704-013-0834-z, 2013.

971 Habib, E., ElSaadani, M., and Haile, A. T.: Climatology-Focused Evaluation of CMORPH and  
972 TMPA Satellite Rainfall Products over the Nile Basin, *Journal of Applied Meteorology*  
973 *and Climatology*, 51, 2105-2121, 10.1175/jamc-d-11-0252.1, 2012a.

974 Habib, E., Haile, A. T., Tian, Y., and Joyce, R. J.: Evaluation of the High-Resolution CMORPH  
975 Satellite Rainfall Product Using Dense Rain Gauge Observations and Radar-Based  
976 Estimates, *Journal of Hydrometeorology*, 13, 1784-1798, 10.1175/jhm-d-12-017.1,  
977 2012b.

978 Habib, E., Haile, A., Sazib, N., Zhang, Y., and Rientjes, T.: Effect of Bias Correction of  
979 Satellite-Rainfall Estimates on Runoff Simulations at the Source of the Upper Blue  
980 Nile, *Remote Sensing*, 6, 6688-6708, 2014.

981 Haile, A. T., Rientjes, T., Gieske, A., and Gebremichael, M.: Rainfall Variability over  
982 Mountainous and Adjacent Lake Areas: The Case of Lake Tana Basin at the Source of  
983 the Blue Nile River, *Journal of Applied Meteorology and Climatology*, 48, 1696-1717,  
984 10.1175/2009JAMC2092.1, 2009.

985 Haile, A. T., Habib, E., and Rientjes, T. H. M.: Evaluation of the climate prediction center CPC  
986 morphing technique CMORPH rainfall product on hourly time scales over the source  
987 of the Blue Nile river, *Hydrological processes*, 27, 1829-1839, 2013.

988 Haile, A. T., Yan, F., and Habib, E.: Accuracy of the CMORPH satellite-rainfall product over  
989 Lake Tana Basin in Eastern Africa, *Atmospheric Research. In Press, Accepted*  
990 *manuscript*, <http://dx.doi.org/10.1016/j.atmosres.2014.11.011>, 2014.

- 991 Haile, A. T., Yan, F., and Habib, E.: Accuracy of the CMORPH satellite-rainfall product over  
 992 Lake Tana Basin in Eastern Africa, *Atmospheric Research*, 163, 177-187,  
 993 <http://dx.doi.org/10.1016/j.atmosres.2014.11.011>, 2015.
- 994 Heidinger, H., Yarlequé, C., Posadas, A., and Quiroz, R.: TRMM rainfall correction over the  
 995 Andean Plateau using wavelet multi-resolution analysis, *International Journal of*  
 996 *Remote Sensing*, 33, 4583-4602, 10.1080/01431161.2011.652315, 2012.
- 997 Hempel, S., Frieler, K., Warszawski, L., Schewe, J., and Piontek, F.: A trend-preserving bias  
 998 correction - the ISI-MIP approach, *Earth Syst. Dynam.*, 4, 219-236, 10.5194/esd-4-219-  
 999 2013, 2013.
- 1000 Hughes, D. A.: Comparison of satellite rainfall data with observations from gauging station  
 1001 networks, *Journal of Hydrology*, 327, 399-410,  
 1002 <http://dx.doi.org/10.1016/j.jhydrol.2005.11.041>, 2006.
- 1003 Ines, A. V. M., and Hansen, J. W.: Bias correction of daily GCM rainfall for crop simulation  
 1004 studies, *Agricultural and Forest Meteorology*, 138, 44-53,  
 1005 <http://dx.doi.org/10.1016/j.agrformet.2006.03.009>, 2006.
- 1006 Jiang, S.-h., Zhou, M., Ren, L.-l., Cheng, X.-r., and Zhang, P.-j.: Evaluation of latest TMPA  
 1007 and CMORPH satellite precipitation products over Yellow River Basin, *Water Science*  
 1008 *and Engineering*, 9, 87-96, <http://dx.doi.org/10.1016/j.wse.2016.06.002>, 2016.
- 1009 Johnson, F. and Sharma, A.: Accounting for interannual variability: A comparison of options  
 1010 for water resources climate change impact assessments, *Water Resour. Res.*, 47(4),  
 1011 <doi:10.1029/2010WR009272>, 2011.
- 1012 Katiraië-Boroujerdy, P., Nasrollahi, N., Hsu, K., and Sorooshian, S.: Evaluation of satellite-  
 1013 based precipitation estimation over Iran, Elsevier, Kidlington, ROYAUME-UNI, 15  
 1014 pp., 2013.
- 1015 Khan, S. I., Hong, Y., Gourley, J. J., Khattak, M. U. K., Yong, B., and Vergara, H. J.:  
 1016 Evaluation of three high-resolution satellite precipitation estimates: Potential for  
 1017 monsoon monitoring over Pakistan, *Advances in Space Research*, 54, 670-684,  
 1018 <http://dx.doi.org/10.1016/j.asr.2014.04.017>, 2014.
- 1019 Koutsouris, A. J., Chen, D., and Lyon, S. W.: Comparing global precipitation data sets in  
 1020 eastern Africa: a case study of Kilombero Valley, Tanzania, *Int. J. Climatol.*, 36, 2000-  
 1021 2014, 10.1002/joc.4476, 2016.
- 1022 Kucuk, U., Eyuboglu, M., Kucuk, H. O. and Degirmencioglu, G.: Importance of using proper  
 1023 post hoc test with ANOVA, *Int. J. Cardiol.*, 209, 346, <doi:10.1016/j.ijcard.2015.11.061>,  
 1024 2018.
- 1025 Leander, R., Buishand, T. A., van den Hurk, B. J. J. M. and de Wit, M. J. M.: Estimated changes  
 1026 in flood quantiles of the river Meuse from resampling of regional climate model output,  
 1027 *J. Hydrol.*, 351(3-4), 331-343, <doi:10.1016/j.jhydrol.2007.12.020>, 2008.
- 1028 Lenderink, G., Buishand, A. and van Deursen, W.: Estimates of future discharges of the river  
 1029 Rhine using two scenario methodologies: direct versus delta approach, *Hydrol. Earth*  
 1030 *Syst. Sci.*, 11(3), 1145-1159, <doi:10.5194/hess-11-1145-2007>, 2007.
- 1031 Li, J., and Heap, A. D.: A review of comparative studies of spatial interpolation methods in  
 1032 environmental sciences: Performance and impact factors, *Ecological Informatics*, 6,  
 1033 228-241, <http://dx.doi.org/10.1016/j.ecoinf.2010.12.003>, 2011.
- 1034 Liu, J., Duan, Z., Jiang, J., and Zhu, A.-X.: Evaluation of Three Satellite Precipitation Products  
 1035 TRMM 3B42, CMORPH, and PERSIANN over a Subtropical Watershed in China,  
 1036 *Advances in Meteorology*, 2015, 13, 10.1155/2015/151239, 2015.
- 1037 Liu, Z.: Comparison of precipitation estimates between Version 7 3-hourly TRMM Multi-  
 1038 Satellite Precipitation Analysis (TMPA) near-real-time and research products,  
 1039 *Atmospheric Research*, 153, 119-133,  
 1040 <http://dx.doi.org/10.1016/j.atmosres.2014.07.032>, 2015.



1041 Lo Conti, F., Hsu, K.-L., Noto, L. V., and Sorooshian, S.: Evaluation and comparison of  
1042 satellite precipitation estimates with reference to a local area in the Mediterranean Sea,  
1043 Atmospheric Research, 138, 189-204,  
1044 <http://dx.doi.org/10.1016/j.atmosres.2013.11.011>, 2014.

1045 Maraun, D.: Bias Correcting Climate Change Simulations - a Critical Review, Current Climate  
1046 Change Reports, 2, 211-220, 10.1007/s40641-016-0050-x, 2016.

1047 Marcos, R., Llasat, M. C., Quintana-Seguí, P., and Turco, M.: Use of bias correction techniques  
1048 to improve seasonal forecasts for reservoirs — A case-study in northwestern  
1049 Mediterranean, Science of The Total Environment, 610–611, 64-74,  
1050 <https://doi.org/10.1016/j.scitotenv.2017.08.010>, 2018.

1051 Matos, J. P., Cohen Liechti, T., Juízo, D., Portela, M. M., and Schleiss, A. J.: Can satellite  
1052 based pattern-oriented memory improve the interpolation of sparse historical rainfall  
1053 records?, Journal of Hydrology, 492, 102-116,  
1054 <http://dx.doi.org/10.1016/j.jhydrol.2013.04.014>, 2013.

1055 Meier, P., Frömel, A., and Kinzelbach, W.: Hydrological real-time modelling in the Zambezi  
1056 river basin using satellite-based soil moisture and rainfall data., Hydrol. Earth Syst.  
1057 Sci., 15, 999-1008, 2011.

1058 Meyer, H., Dröner, J., and Nauss, T.: Satellite-based high-resolution mapping of rainfall over  
1059 southern Africa, Atmos. Meas. Tech., 10, 2009-2019, 10.5194/amt-10-2009-2017,  
1060 2017.

1061 Moazami, S., Golian, S., Kavianpour, M. R., and Hong, Y.: Comparison of PERSIANN and  
1062 V7 TRMM Multi-satellite Precipitation Analysis (TMPA) products with rain gauge  
1063 data over Iran, International Journal of Remote Sensing, 34, 8156-8171,  
1064 10.1080/01431161.2013.833360, 2013.

1065 Müller, M. F., and Thompson, S. E.: Bias adjustment of satellite rainfall data through stochastic  
1066 modeling: Methods development and application to Nepal, Advances in Water  
1067 Resources, 60, 121-134, <http://dx.doi.org/10.1016/j.advwatres.2013.08.004>, 2013.

1068 Najmaddin, P. M., Whelan, M. J., and Balzter, H.: Application of Satellite-Based Precipitation  
1069 Estimates to Rainfall-Runoff Modelling in a Data-Scarce Semi-Arid Catchment,  
1070 Climate, 5, 32, 2017.

1071 NIST/SEMATECH: e-handbook of statistical methods. Croarkin, C., Tobias, P., and Zey, C.  
1072 (Eds.), NIST ;, [Gaithersburg, Md.] :, 2001.

1073 Pereira Filho, A. J., Carbone, R. E., Janowiak, J. E., Arkin, P., Joyce, R., Hallak, R., and Ramos,  
1074 C. G. M.: Satellite Rainfall Estimates Over South America – Possible Applicability to  
1075 the Water Management of Large Watersheds1, JAWRA Journal of the American Water  
1076 Resources Association, 46, 344-360, 10.1111/j.1752-1688.2009.00406.x, 2010.

1077 Rientjes, T., Haile, A. T., and Fenta, A. A.: Diurnal rainfall variability over the Upper Blue  
1078 Nile Basin: A remote sensing based approach, International Journal of Applied Earth  
1079 Observation and Geoinformation, 21, 311-325,  
1080 <http://dx.doi.org/10.1016/j.jag.2012.07.009>, 2013a.

1081 Rientjes, T. H. M., Muthuwatta, L. P., Bos, M. G., Booij, M. J., and Bhatti, H. A.: Multi-  
1082 variable calibration of a semi-distributed hydrological model using streamflow data and  
1083 satellite-based evapotranspiration, Journal of Hydrology, 505, 276-290,  
1084 <http://dx.doi.org/10.1016/j.jhydrol.2013.10.006>, 2013b.

1085 Romano, F., Cimini, D., Nilo, S., Di Paola, F., Ricciardelli, E., Ripepi, E., and Viggiano, M.:  
1086 The Role of Emissivity in the Detection of Arctic Night Clouds, Remote Sensing, 9,  
1087 406, 2017.

1088 Romilly, T. G., and Gebremichael, M.: Evaluation of satellite rainfall estimates over Ethiopian  
1089 river basins, Hydrol. Earth Syst. Sci., 15, 1505-1514, 10.5194/hess-15-1505-2011,  
1090 2011.

1091 Seo, D. J., Breidenbach, J. P., and Johnson, E. R.: Real-time estimation of mean field bias in  
1092 radar rainfall data, *Journal of Hydrology*, 223, 131-147,  
1093 [http://dx.doi.org/10.1016/S0022-1694\(99\)00106-7](http://dx.doi.org/10.1016/S0022-1694(99)00106-7), 1999.

1094 Shrestha, M. S.: Bias-adjustment of satellite-based rainfall estimates over the central  
1095 Himalayas of Nepal for flood prediction. PhD thesis, Kyoto University, 2011.

1096 Smiatek, G., Kunstmann, H., and Senatore, A.: EURO-CORDEX regional climate model  
1097 analysis for the Greater Alpine Region: Performance and expected future change,  
1098 *Journal of Geophysical Research: Atmospheres*, 121, 7710-7728,  
1099 10.1002/2015JD024727, 2016.

1100 Srivastava, P. K., Islam, T., Gupta, M., Petropoulos, G., and Dai, Q.: WRF Dynamical  
1101 Downscaling and Bias Correction Schemes for NCEP Estimated Hydro-Meteorological  
1102 Variables, *Water Resources Management*, 29, 2267-2284, 10.1007/s11269-015-0940-  
1103 z, 2015.

1104 Switanek, M. B., Troch, P. A., Castro, C. L., Leuprecht, A., Chang, H. I., Mukherjee, R., and  
1105 Demaria, E. M. C.: Scaled distribution mapping: a bias correction method that preserves  
1106 raw climate model projected changes, *Hydrol. Earth Syst. Sci.*, 21, 2649-2666,  
1107 10.5194/hess-21-2649-2017, 2017.

1108 Taylor, K. E.: Summarizing multiple aspects of model performance in a single diagram, *Journal*  
1109 *of Geophysical Research: Atmospheres*, 106, 7183-7192, 10.1029/2000JD900719,  
1110 2001.

1111 Tesfagiorgis, K., Mahani, S. E., Krakauer, N. Y., and Khanbilvardi, R.: Bias correction of  
1112 satellite rainfall estimates using a radar-gauge product &ndash; a case study in  
1113 Oklahoma (USA), *Hydrol. Earth Syst. Sci.*, 15, 2631-2647, 10.5194/hess-15-2631-  
1114 2011, 2011.

1115 Themeßl, M. J., Gobiet, A., and Heinrich, G.: Empirical-statistical downscaling and error  
1116 correction of regional climate models and its impact on the climate change signal, *Clim.*  
1117 *Change*, 112, 449-468 2012.

1118 Thiemiig, V., Rojas, R., Zambrano-Bigiarini, M., Levizzani, V., and De Roo, A.: Validation of  
1119 Satellite-Based Precipitation Products over Sparsely Gauged African River Basins,  
1120 *Journal of Hydrometeorology*, 13, 1760-1783, 10.1175/jhm-d-12-032.1, 2012.

1121 Thiemiig, V., Rojas, R., Zambrano-Bigiarini, M., and De Roo, A.: Hydrological evaluation of  
1122 satellite-based rainfall estimates over the Volta and Baro-Akobo Basin, *Journal of*  
1123 *Hydrology*, 499, 324-338, 10.1016/j.jhydrol.2013.07.012, 2013.

1124 Thorne, V., Coakeley, P., Grimes, D., and Dugdale, G.: Comparison of TAMSAT and CPC  
1125 rainfall estimates with raingauges, for southern Africa, *International Journal of Remote*  
1126 *Sensing*, 22, 1951-1974, 10.1080/01431160118816, 2001.

1127 Tian, Y., Peters-Lidard, C. D., and Eylander, J. B.: Real-Time Bias Reduction for Satellite-  
1128 Based Precipitation Estimates, *Journal of Hydrometeorology*, 11, 1275-1285,  
1129 10.1175/2010JHM1246.1, 2010.

1130 Tobin, K. J., and Bennett, M. E.: Adjusting Satellite Precipitation Data to Facilitate Hydrologic  
1131 Modeling, *Journal of Hydrometeorology*, 11, 966-978, doi:10.1175/2010JHM1206.1,  
1132 2010.

1133 Toté, C., Patricio, D., Boogaard, H., van der Wijngaart, R., Tarnavsky, E., and Funk, C.:  
1134 Evaluation of Satellite Rainfall Estimates for Drought and Flood Monitoring in  
1135 Mozambique, *Remote Sensing*, 7, 1758, 2015.

1136 Tsidu, G. M.: High-Resolution Monthly Rainfall Database for Ethiopia: Homogenization,  
1137 Reconstruction, and Gridding, *Journal of Climate*, 25, 8422-8443, 10.1175/JCLI-D-12-  
1138 00027.1, 2012.

1139 Tumbare, M. J.: Management of River Basins and Dams: The Zambezi River Basin, edited by:  
1140 Tumbare, M. J., Taylor & Francis, 318 pp., 2000.

1141 Tumbare, M. J.: The Management of the Zambezi River Basin and Kariba Dam, Bookworld  
1142 Publishers, Lusaka, 2005.

1143 Valdés-Pineda, R., Demaría, E. M. C., Valdés, J. B., Wi, S., and Serrat-Capdevilla, A.: Bias  
1144 correction of daily satellite-based rainfall estimates for hydrologic forecasting in the  
1145 Upper Zambezi, Africa, *Hydrol. Earth Syst. Sci. Discuss.*, 2016, 1-28, 10.5194/hess-  
1146 2016-473, 2016.

1147 Vernimmen, R. R. E., Hooijer, A., Mamenun, Aldrian, E., and van Dijk, A. I. J. M.: Evaluation  
1148 and bias correction of satellite rainfall data for drought monitoring in Indonesia, *Hydrol.*  
1149 *Earth Syst. Sci.*, 16, 133-146, 10.5194/hess-16-133-2012, 2012.

1150 Wehbe, Y., Ghebreyesus, D., Temimi, M., Milewski, A., and Al Mandous, A.: Assessment of  
1151 the consistency among global precipitation products over the United Arab Emirates,  
1152 *Journal of Hydrology: Regional Studies*, 12, 122-135,  
1153 <https://dx.doi.org/10.1016/j.ejrh.2017.05.002>, 2017.

1154 Wilks, D.: *Statistical Methods in the Atmospheric Sciences*, 2nd ed., Academic Press,  
1155 Burlington, Mass, 2006.

1156 Woody, J., Lund, R., and Gebremichael, M.: Tuning Extreme NEXRAD and CMORPH  
1157 Precipitation Estimates, *Journal of Hydrometeorology*, 15, 1070-1077, 10.1175/jhm-d-  
1158 13-0146.1, 2014.

1159 World Bank: *The Zambezi River Basin : A Multi-Sector Investment Opportunities Analysis -*  
1160 *Summary Report*. World Bank. © World Bank.  
1161 <https://openknowledge.worldbank.org/handle/10986/2958> License: Creative  
1162 Commons Attribution CC BY 3.0., 2010a.

1163 World Bank: *The Zambezi River Basin: A Multi-Sector Investment Opportunities Analysis,*  
1164 *Volume 2 Basin Development Scenarios*, 2010b.

1165 Worqlul, A. W., Maathuis, B., Adem, A. A., Demissie, S. S., Langan, S., and Steenhuis, T. S.:  
1166 Comparison of rainfall estimations by TRMM 3B42, MPEG and CFSR with ground-  
1167 observed data for the Lake Tana basin in Ethiopia, *Hydrol. Earth Syst. Sci.*, 18, 4871-  
1168 4881, 10.5194/hess-18-4871-2014, 2014.

1169 Wu, L., and Zhai, P.: Validation of daily precipitation from two high-resolution satellite  
1170 precipitation datasets over the Tibetan Plateau and the regions to its east, *Acta Meteorol*  
1171 *Sin*, 26, 735-745, 10.1007/s13351-012-0605-2, 2012.

1172 Yang, X., Xie, X., Liu, D. L., Ji, F., and Wang, L.: Spatial Interpolation of Daily Rainfall Data  
1173 for Local Climate Impact Assessment over Greater Sydney Region, *Advances in*  
1174 *Meteorology*, 2015, 12, 10.1155/2015/563629, 2015.

1175 Yin, Z. Y., Zhang, X., Liu, X., Colella, M., and Chen, X.: An assessment of the biases of  
1176 satellite rainfall estimates over the tibetan plateau and correction methods based on  
1177 topographic analysis, *Journal of Hydrometeorology*, 9, 301, 2008.

1178 Yoo, C., Park, C., Yoon, J., and Kim, J.: Interpretation of mean-field bias correction of radar  
1179 rain rate using the concept of linear regression, *Hydrological Processes*, 28, 5081-5092,  
1180 10.1002/hyp.9972, 2014.

1181 Zulkafli, Z., Buytaert, W., Onof, C., Manz, B., Tarnavsky, E., Lavado, W., and Guyot, J.-L.: A  
1182 Comparative Performance Analysis of TRMM 3B42 (TMPA) Versions 6 and 7 for  
1183 Hydrological Applications over Andean–Amazon River Basins, *Journal of*  
1184 *Hydrometeorology*, 15, 581-592, doi:10.1175/JHM-D-13-094.1, 2014.

1185  
1186  
1187  
1188

1189 **Appendix 1:** Rain gauge stations in the Zambezi subbasins showing x and y location, subbasin they belong to, year of data

1190 availability, % of missing gaps, station elevation and distance from large-scale water bodies.

Station	Subbasin	Zambezi classification	X Coord	Y Coord	Start date	End Date	% gaps (missing records)	Elevation (m)	Distance from lake (km)
Marromeu	Zambezi	Lower	36.95	-18.28	29/05/2007	31/12/2013	0.37	3	90
	Delta	Zambezi				31/12/2013			265
Caia	Zambezi	Lower	35.38	-17.82	29/05/2007	31/12/2013	0.13	28	157
	Delta	Zambezi							
Nsanje	Shire	Lower	35.27	-16.95	01/01/1998	31/12/2013	3.49	39	113
	Zambezi	Lower							
Makhanga	Shire	Zambezi	35.15	-16.52	01/01/1998	31/12/2013	9.43	48	96
	Shire	Lower							
Nchalo	Zambezi	Lower	34.93	-16.23	01/01/1998	31/12/2013	0.60	64	123
	Shire	Lower							
Ngabu	Zambezi	Lower	34.95	-16.50	01/01/1998	31/12/2010	0.74	89	77
	Shire	Lower							
Chikwawa Tete (Chingodzi)	Zambezi	Lower	34.78	-16.03	01/01/1998	31/12/2010	0.93	107	135
	Tete	Lower							
Chingodzi	Zambezi	Lower	33.58	-16.18	29/05/2007	31/12/2013	0.17	151	101
	Shire	Lower							
Zumbo	Zambezi	Lower	34.63	-16.00	29/05/2007	10/01/2013	11.8	280	<5
	Shire	Lower							
Mushumbi	Zambezi	Middle	30.45	-15.62	29/05/2007	12/09/2012	0.16	345	43
	Kariba	Middle							
Kanyemba	Zambezi	Middle	30.56	-16.15	11/06/2008	11/12/2013	7.47	369	<5
	Tete	Middle							
Morumbala	Zambezi	Lower	30.42	-15.63	01/01/1998	30/03/2013	5.86	372	206
	Zambezi	Lower							
Mágoè	Delta	Zambezi	35.58	-17.35	29/05/2007	10/01/2013	13.3	378	10
	Tete	Middle							
Muzarabani	Zambezi	Middle	31.75	-15.82	01/01/2009	31/12/2013	9.6	427	49
	Tete	Middle							
Monkey	Zambezi	Lower	31.01	-16.39	01/01/1998	31/12/2013	1.14	430	<5
	Shire	Lower							
Mangochi	Zambezi	Lower	34.92	-14.08	01/01/1998	30/11/2010	0.00	478	<5
	Shire	Lower							
Rukomechi	Zambezi	Middle	35.25	-14.47	01/01/1998	31/12/2010	0.02	481	68
	Kariba	Middle							
Mutarara	Zambezi	Lower	29.38	-16.13	01/01/1998	31/12/2013	6.40	530	201
	Shire	Lower							
Mfuwe	Zambezi	Middle	33.00	-17.38	29/05/2007	10/01/2013	11.7	548	246
	Luangwa	Middle							
Mimosa	Zambezi	Lower	31.93	-13.27	01/01/1998	31/12/2010	2.70	567	72
	Shire	Lower							
Kariba	Zambezi	Middle	35.62	-16.07	01/01/1998	31/12/2010	3.96	616	21
	Kariba	Middle							
Balaka	Zambezi	Lower	28.80	-16.52	01/01/1998	31/12/2013	0.01	618	24
	Shire	Lower							
Thyolo	Zambezi	Lower	34.97	-14.98	01/01/1998	30/04/2010	0.78	618	86
	Shire	Lower							
Chileka	Zambezi	Middle	35.13	-16.13	01/01/1998	31/12/2010	0.11	624	64
	Shire	Lower							
Fingoe Muze	Zambezi	Middle	34.97	-15.67	01/01/1998	31/12/2013	0.60	744	44
	Tete	Middle							
Neno	Zambezi	Lower	31.88	-15.17	01/01/2009	31/12/2013	5.9	881	75
	Tete	Zambezi							
Zámbugue	Zambezi	Lower	31.38	-14.95	01/01/2009	31/12/2013	8.8	888	64
	Shire	Lower							
Mt Darwin	Zambezi	Middle	34.65	-15.40	01/01/1998	01/01/2010	9.14	903	56
	Tete	Middle							
	Zambezi	Middle	30.80	-15.11	01/01/2009	31/12/2013	9.8	950	94
	Tete	Middle							
	Zambezi	Lower	31.58	-16.78	01/01/1998	02/03/2008	5.00	962	

Chipata	Shire	Lower Zambezi	32.58	-13.55	01/01/1998	13/08/2003	1.11	995	179
Makoka	Shire	Lower Zambezi	35.18	-15.53	01/01/1998	31/12/2010	0.00	996	27
Livingstone	Kariba	Middle Zambezi	25.82	-17.82	01/01/1998	31/12/2013	0.00	996	107
Senanga	Barotse	Upper Zambezi	23.27	-16.10	01/01/1998	31/12/2013	8.90	1001	444
Petauke	Luangwa	Middle Zambezi	31.28	-14.25	01/02/1998	31/12/2013	0.40	1006	155
Msekera	Luangwa	Middle Zambezi	32.57	-13.65	01/03/1998	31/12/2015	19.7	1028	179
Kalabo	Lungue	Upper Zambezi	22.70	-14.85	01/01/1998	31/12/2011	5.20	1033	582
Mongu	Bungo	Upper Zambezi	23.15	-15.25	01/01/1998	31/12/2013	0.51	1052	518
Kasungu	Shire	Lower Zambezi	33.47	-13.02	01/01/2003	31/07/2013	0.00	1063	89
Victoria Falls	Kariba	Middle Zambezi	25.85	-18.10	01/01/1998	31/12/2013	2.26	1065	107
Bolero	Luangwa	Middle Zambezi	33.78	-11.02	01/01/2003	31/05/2013	0.00	1070	38
Pandamatenga	Kariba	Middle Zambezi	25.63	-18.53	01/01/1998	31/12/2013	0.01	1071	151
Zambezi	Lungue	Upper Zambezi	23.12	-13.53	01/01/1998	31/12/2013	1.60	1075	611
Kabompo	Bungo	Upper Zambezi	24.20	-13.60	01/01/1998	30/04/2005	0.08	1086	505
Chichiri	Shire	Lower Zambezi	35.05	-15.78	01/01/1998	31/12/2010	0.00	1136	40
Chitedze	Shire	Lower Zambezi	33.63	-13.97	01/01/2003	30/04/2013	0.00	1150	84
Lundazi	Luangwa	Middle Zambezi	33.20	-12.28	01/01/2003	30/04/2013	1.40	1151	91
Guruve	Tete	Middle Zambezi	30.70	-16.65	01/01/1998	30/03/2013	0.02	1159	86
Kaoma	Barotse	Upper Zambezi	24.80	-14.80	01/01/1998	31/11/2013	9.89	1162	358
Bvumbwe	Shire	Lower Zambezi	35.07	-15.92	01/01/1998	01/01/2011	0.00	1172	59
Kasempa	Kafue	Middle Zambezi	25.85	-13.53	01/01/1998	31/12/2013	9.10	1185	431
Kabwe	Luangwa	Middle Zambezi	28.47	-14.45	01/01/1998	13/10/2012	1.54	1209	230
Chitipa	Shire	Lower Zambezi	33.27	-9.70	01/01/2003	06/01/2013	0.05	1288	62
Mwinilunga	Kabompo	Upper Zambezi	24.43	-11.75	01/01/1998	31/12/2013	4.81	1319	520
Karoi	Tete	Middle Zambezi	29.62	-16.83	01/01/1998	31/12/2004	15.08	1345	88
Solwezi	Kafue	Middle Zambezi	26.38	-12.18	01/01/1998	31/12/2013	0.02	1372	356
Harare (Belvedere)	Tete	Middle Zambezi	31.02	-17.83	01/01/1998	31/03/2013	7.80	1472	209
Harare(Kutsaga)	Tete	Middle Zambezi	31.13	-17.92	01/01/2004	30/09/2010	0.55	1488	209
Mvurwi	Tete	Middle Zambezi	30.85	-17.03	01/01/1998	11/12/2000	0.00	1494	102
Dedza	Shire	Lower Zambezi	34.25	-14.32	01/01/2003	31/10/2012	0.00	1575	44

1191  
1192  
1193  
1194

1195  
1196  
1197  
1198

**Appendix 2:** Bias correction scheme based Taylor Diagram performance indicators (correlation coefficients, standard deviations and RMSE) of rain gauge (reference) vs CMORPH estimations (corrected and uncorrected), period 1998-2013, for Lower, Middle and Upper Zambezi Basin.

Subbasin	Rainfall estimate	RMSE (mm/day)	Correlation Coefficient	Standard Deviation (mm/day)
Lower Zambezi	Gauge			9.38
	R-CMORPH	9.98	0.46	8.00
	PT	10.41	0.57	8.52
	QME	9.15	0.55	6.98
	EZ	10.48	0.62	6.35
	DT	9.30	0.56	6.55
	STB	8.59	0.72	7.17
Middle Zambezi	Gauge			7.94
	R-CMORPH	8.12	0.49	7.44
	PT	7.87	0.62	6.84
	QME	7.51	0.60	6.00
	EZ	10.69	0.65	6.93
	DT	8.04	0.59	6.96
	STB	7.49	0.76	6.81
Upper Zambezi	Gauge			8.29
	R-CMORPH	7.23	0.45	6.60
	PT	7.97	0.62	7.29
	QME	8.05	0.55	7.12
	EZ	11.50	0.60	8.13
	DT	7.85	0.55	6.45
	STB	0.54	0.74	7.29

1199  
1200